UCRL-17068

University of California

Ernest O. Lawrence Radiation Laboratory

STUDY OF BRANCH POINTS IN THE ANGULAR MOMENTUM PLANE

TWO-WEEK LOAN COPY

This is a Library Circulating Copy which may be borrowed for two weeks. For a personal retention copy, call Tech. Info. Division, Ext. 5545

Berkeley, California

DISCLAIMER

This document was prepared as an account of work sponsored by the United States Government. While this document is believed to contain correct information, neither the United States Government nor any agency thereof, nor the Regents of the University of California, nor any of their employees, makes any warranty, express or implied, or assumes any legal responsibility for the accuracy, completeness, or usefulness of any information, apparatus, product, or process disclosed, or represents that its use would not infringe privately owned rights. Reference herein to any specific commercial product, process, or service by its trade name, trademark, manufacturer, or otherwise, does not necessarily constitute or imply its endorsement, recommendation, or favoring by the United States Government or any agency thereof, or the Regents of the University of California. The views and opinions of authors expressed herein do not necessarily state or reflect those of the United States Government or any agency thereof or the Regents of the University of California.

UCRL-17068

UNIVERSITY OF CALIFORNIA
Lawrence Radiation Laboratory
Berkeley, California

AEC Contract No. W-7405-eng-48

STUDY OF BRANCH POINTS IN THE ANGULAR MOMENTUM PLANE

Heinz J. Rothe

(Ph. D. Thesis)

August 24, 1966

Table of Contents

Page

Abstract v

Introduction 1

I. Connection Between Angular Momentum Cuts and the Asymptotic Behaviour of the Amplitude 9

II. The Single Regge Pole Exchange Diagram 14

1. The AFS Approximation 14

2. Representation of the AFS Amplitude as a Contour Integral in the Energy Plane of the Exchanged Regge Pole 18

3. Location of the Singularities in the j Plane 22

4. Formulae for the Discontinuities of $c(u,s)$, and Asymptotic Behaviour of the AFS Amplitude 29

5. Evaluation of $c(u,s)$ 34

6. Concluding Remarks and Summary 45

7. Cancellation of the Cuts 51

III. The Double Regge Pole Exchange Diagram 54

1. The AFS Approximation, and Location of the Singularities in the j Plane 54

2. Asymptotic Behaviour of the AFS Amplitude 60

3. Concluding Remarks and Summary 65

IV. Diagrams That Have the Mandelstam Singularities 71

1. An Estimate of the Contribution Coming from the Leading Angular Momentum Branch Point of the Double Regge Pole Exchange Diagram 78

2. Conclusion 84

Page

Aknowledgments 87

Appendix 88

Footnotes and References 92

Figure Captions 95

STUDY OF BRANCH POINTS IN THE ANGULAR MOMENTUM PLANE

Heinz J. Rothe

Lawrence Radiation Laboratory
University of California
Berkeley, California

August 24, 1966

ABSTRACT

A study is made of the Amati, Fubini, Stanghellini (AFS) type of approximation to the amplitudes associated with the exchange of a single Regge pole and an elementary spinless particle, and of two Regge poles, respectively. The location, motion, and nature of the singularities in the complex angular momentum plane of the s reaction which appear in these approximations, and their cancellation in the full diagram, are considered in detail; the singularities are found to be of two general types: branch points whose positions are independent of particle masses, and those which depend on them. Only the former ones determine the asymptotic behaviour of the AFS amplitudes in the physical scattering region, while the latter singularities appear only on the physical sheet via the mass-independent branch points at unphysical momentum transfers. The same method used in the study of the AFS approximation to the diagrams which do not have the AFS-type singularities is applied to the analysis of the Mandelstam diagrams for which the above-mentioned cancellation of the cuts does not occur. The analysis, although less rigorous, suggests that the

location and nature of the singularities in the j plane are the same as those found for the AFS type of approximations to their simpler versions. With a number of approximations which, although plausible, are hard to justify rigorously, an estimate is made of the relative contributions to the amplitude coming from the angular momentum cut and the corresponding Regge pole.

INTRODUCTION

It was originally noticed by Amati, Fubini, and Stanghellini (AFS) that if one combines two Regge poles according to two-body unitarity in the t channel (as indicated by the dashed line in Fig. 3), and then disperses the resultant absorptive part in t, one arrives at an amplitude which exhibits moving branch points in the angular momentum plane.[1] Although the cuts suggested by AFS were later found by Mandelstam to be absent in the diagram considered by them,[2] these cuts are nevertheless believed to be present in more complicated diagrams such as the ones shown in Figs. 2 and 4 (see references 2, 4, 5, 8); their crucial feature is the appearance of the crossed lines. The presence of the Mandelstam cuts is the result of inelastic contributions to the unitarity relation, and is particular to the relativistic problem (for potential scattering the crossed graphs do not occur). If such singularities indeed exist then they cannot be ignored, since it was shown by the above authors that their contribution to the amplitude at large t is similar to that of a Regge pole (except for logarithmic factors), where the trajectory function $\alpha(s)$ is replaced by $\lambda(s)$:

$$\lambda(s) = 2\alpha(s/4) - 1 \quad .$$

(Actually, AFS did not write it in this form; we shall see, however, that the above expression for $\lambda(s)$ is rigorously true). Thus if $\alpha(s)$ is the Pomeranchuk trajectory, for example, then the branch

point will coincide with the position of the Pomeranchuk pole at $s = 0$ (i.e., in the forward direction), while for $s \lesssim 0$ and large t, the cut will dominate over the pole. If on the other hand $\alpha(0) = 1 - \epsilon$, then there exists a region of small momentum transfers where the pole will dominate over the cut. For s sufficiently negative, however, the situation might very well get turned around, with the cut giving the dominant contribution. In addition it was indicated by Mandelstam[2] and shown by Gribov et al.[5] that the generalization of $\lambda(s) = 2\alpha(s/4) - 1$ to the case where we exchange n identical Regge poles is

$$\lambda_n(s) = n\,\alpha(s/n^2) - n + 1 ,$$

which shows that the trajectories $\lambda_n(s)$ become flatter as we increase n. Thus, if $\alpha(s)$ is the Pomeranchuk trajectory, for example, then the above singularities could dominate even more strongly than the singularity at $\lambda = 2\alpha(s/4) - 1$ the contribution from the Pomeranchuk pole for all negative momentum transfers (unless we are dealing with very weak branch points). The above discussion was concerned with angular momentum branch points that arise from the multiple exchange of identical trajectories. In general one will, of course, have to consider the contribution to the amplitude coming from the exchange of different trajectories; the location of the associated angular momentum branch points, however, can no longer be given by a simple formula such as the one discussed above. In view of what has been

said above, it is desirable to get as clear an understanding as possible regarding the existence or nonexistence of these cuts in various types of diagrams, the location and nature of the various branch points one is dealing with, and, if possible, the strength of the discontinuities involved.

Let us now review in more detail the history of branch points in the angular momentum plane. Following the suggestion of Amati, Fubini, and Stanghellini that the continued partial-wave amplitude is not a meromorphic function of the angular momentum, Mandelstam analyzed a modified version of the AFS diagram (see Fig. 1), and shown that the cuts suggested by the above authors were merely the result of a poor approximation to the unitarity relation. At the same time he was able to show that in a certain approximation (to be discussed below) the diagram of Fig. 2 does give rise to a branch point in the angular momentum plane whose location is identical to that obtained from an AFS type of approximation to the corresponding diagram of Fig. 1.[2] The essential features of Fig. 2 are its right- and left-hand portions (i.e., the "crosses") which when considered by themselves exhibit a third double spectral function with respect to the s reaction. The proof of the above result is rather involved. It seems worthwhile, however, to give a brief summary of the general method used, which leaves little to offer where ingenuity is concerned. Rather than making an elastic unitarity approximation with respect to the t reaction in the diagram of Fig. 1 (which would be the analog of the AFS procedure in connection with the diagram of Fig. 3),

Mandelstam applies three body unitarity to the s channel. By a clever choice of variables for the three-body intermediate state, and equipped with the knowledge of the singularity structure of each half of the diagram, Mandelstam is able to show from the large t behaviour of the amplitude that the AFS singularity is absent from the diagram, at least in the three-body unitarity approximation. The method used in the proof depends strongly on the fact that the left- and right-hand portions of the diagram do not possess a third double spectral function in the above-mentioned sense; the method therefore cannot be extended to the diagram of Fig. 2. In order to establish the existence of the singularity in the latter diagram, Mandelstam makes use of the fact that if there exists a bound state or resonance of spin σ lying on the Regge trajectory, then the diagram will have a Gribov-Pomeranchuk singularity at $j = \sigma - 1$, where j is the angular momentum in the s reaction (the elementary exchange is taken to have zero spin, for simplicity). He is then able to show, by a number of ingenious tricks, that the singularity can be made to disappear by moving the AFS cut past the point $j = \sigma - 1$; such a phenomenon, of course, requires that the angular momentum plane exhibit a sheet structure.[3]

The above-mentioned method, once again, cannot be used to either prove or disprove the existence of the angular momentum cut for diagrams of the type shown in Figs. 5 and 6, since they do not possess the Gribov-Pomeranchuk singularity. It was shown subsequently by Wilkin that if the cut is to exist, both the right- and left-hand

portions of the diagram must possess a third double spectral function in the sense that we have mentioned previously.[4] Wilkin's method consisted in treating the various diagrams as Feynman graphs, thus avoiding the complications introduced by multiparticle unitarity. Upon approximating the integrand of the Feynman integral in question by its leading terms at large energies, and subsequently examining its analytic structure, Wilkin finds that unless both the right- and left-hand portions of the diagram possess a third double spectral function, one may distort the integration contours in such a manner that the Regge pole never assumes its characteristic asymptotic form anywhere along the path of integration; with the amplitude vanishing like $1/t^2$ for $t \to \infty$, he then concludes that the AFS singularity must be absent in such diagrams. Although this method is quite general, it nevertheless does not provide us with a deeper understanding of just how the AFS cut is generated, and of the mechanism responsible for its cancellation.

Several other authors have investigated the moving branch points in the angular momentum plane. Thus Gribov et al.[5] considered the possibility of establishing these branch points directly from the structure of the multiparticle unitarity condition for the partial-wave amplitude continued to complex angular momenta j. On the basis of a definite assumption regarding the form of this analytic continuation, they are able to obtain, among other results, the above singularity at $j = 2\alpha(s/4) - 1$ for the double Regge pole exchange case, and its generalization to the exchange of n Regge poles: $j_n = n\,\alpha(s/n^2) - n + 1$.

In addition they conjecture a formula for the discontinuity across the above-mentioned branch point which has the general form of a unitarity relation involving the amplitudes for the production of particles with complex spin (that is, Regge poles).[6] The singularities associated with the exchange of one or two Regge poles have been further considered by Simonov[7] using the form of the many-particle unitarity relation for complex j proposed by Gribov et al. An alternative approach has been proposed by Polkinghorne,[8] who has analyzed the diagram of Fig. 2 using the Feynman parametric representation of the amplitude; in this approach Regge cuts result from pinches in the interior of the hyper-contour of integration where the coefficient of the asymptotic variable t vanishes.[9] The absence of the AFS-type singularities in the diagrams of Figs. 1 and 3, and their presence in the diagrams of Figs. 2 and 4, can, for all of the above approaches, be ultimately stated in terms of the absence or presence of the already mentioned third double spectral function, a fact which had originally been suggested by Mandelstam.[2]

Our interest in the present work was stimulated during a study of the various types of corrections to approximate scattering amplitudes, and their relation to the Regge pole picture; we are referring here in particular to the absorption model of Gottfried and Jackson, and to the Glauber shadow term which arises in connection with scattering from the deuteron. Both types of corrections suggest that in their Reggeized versions they correspond to AFS-type of approximations to the diagrams of Figs. 3 and 7.[10] Now, as we have already emphasized, Mandelstam

(and others) have shown that there must exist another contribution to the scattering amplitude which precisely cancels the above correction terms. This suggests that the correction formulae should be expected to hold only at energies below those at which Regge expansions are legitimate. In any event, it is undoubtedly of great interest to understand the generation of the AFS cut and its cancellation in as much detail as possible. We shall mainly concentrate in this paper on the detailed study of the branch points in the angular momentum plane which occur in the AFS type of approximations to the diagrams of Figs. 1 and 3. The philosophy behind this approach is that we expect the location of the j-plane singularities here, as well as their general nature (that is, square root type, logarithmic type, etc) to be the same as for the diagrams of Figs. 2 and 4.

The organization of the paper will be as follows: in Section I we establish the connection between the asymptotic behaviour of the amplitude and the existence of branch points in the angular momentum plane. We also review the method of Amati, Fubini, and Stanghellini which led to the appearance of an angular momentum cut.

In Section II we extract the leading, large-t, contribution to the Feynman amplitude corresponding to the diagram of Fig. 1, and show that the AFS approximation is equivalent to ignoring certain singularities of the integrand. We then proceed to write the amplitude as a contour integral in the energy plane of the Regge pole and analyze the analytic structure of the integrand (for which an explicit expression is given) in great detail. The nature of the branch points

is established, and the discontinuities across the various cuts are evaluated; we then obtain the correct form for the asymptotic behaviour in t of the AFS amplitude, and conclude the section with an exhibition of the mechanism which is responsible for the cancellation of the cuts, and with some general remarks.

In Section III we make a similar analysis of the diagram involving the exchange of two Regge poles.

Finally, in Section IV, we consider the more complicated diagrams of Figs. 2 and 4, which, as originally suggested by Mandelstam,[2] actually have the AFS-type singularities. Their analysis is, of course, substantially more complicated and we have to make a number of approximations, which, although plausible, are hard to justify rigorously; however, they do lead to the expected results, and allow at least an estimate of the contribution coming from the angular momentum cut.

I. CONNECTION BETWEEN ANGULAR MOMENTUM CUTS AND THE ASYMPTOTIC BEHAVIOUR OF THE AMPLITUDE

Before examining the AFS approximation to the diagram of Fig. 1 which gives rise to cuts in the angular momentum plane, we wish to investigate very briefly how such cuts manifest themselves in the scattering amplitude; this is necessary if we are to make the proper identifications in the subsequent work.

Consider the partial-wave expansion of the invariant amplitude of + or - signature, $A^{\pm}(s,z_s)$, with respect to the s reaction

$$A^{\pm}(s,z_s) = \sum_j (2j+1)\, a_j^{\pm}(s)\, P_j(z_s) , \qquad (I.1)$$

where s is the square of the center of mass (c.m.) energy, and z_s is the cosine of the c.m. scattering angle. $A^{\pm}(s,z_s)$ is defined in terms of the t-channel and u-channel absorptive parts as follows:

$$A^{\pm}(s,z_s) = \frac{1}{\pi}\int_{t_0}^{\infty} dt' \, \frac{A_t(s,t')}{t'-t(s,z_s)} \pm \frac{1}{\pi}\int_{u_0}^{\infty} du' \, \frac{A_u(s,u')}{u'-u(s,-z_s)} .$$

Here t_0 and u_0 are the t-channel and u-channel thresholds respectively. The full amplitude is then related to $A^{\pm}(s,z_s)$ according to

$$A(s,z_s) = \frac{1}{2}\sum_{\sigma} [A^{\sigma}(s,z_s) + \eta_{\sigma} A^{\sigma}(s,-z_s)] , \qquad (I.2)$$

where σ = + or - , and $\eta_{\pm} = \pm 1$. Using the Froissart-Gribov

prescription, one then obtains the continuation of $a_j^{\pm}(s)$ to complex j in the usual manner; we denote the continuation of $a_j^{\pm}(s)$ by $a^{\pm}(j,s)$. Performing a Sommerfeld-Watson transformation on the right-hand side of (I.1), we arrive at the well known integral representation

$$A^{\pm}(s,z_s) = \frac{i}{2} \int_C dj(2j+1)\, a^{\pm}(j,s) \frac{P_j(-z_s)}{\sin \pi j} \tag{I.3}$$

where the contour C encircles the poles of $1/\sin \pi j$ at $j = 0,1,2,\cdots$; for concreteness sake let us assume that $a^{\pm}(j,s)$ is an analytic function of j except for a pole at $j = \alpha^{\pm}(s)$, and a branch point at $j = b^{\pm}(s)$. Equation (I.3) can then be written in the following way [making the usual assumptions regarding $a^{\pm}(j,s)$]:

$$A^{\pm}(s,z_s) = \frac{i}{2} \int_{C_{\pm}} dj(2j+1)\, a^{\pm}(j,s) \frac{P_j(-z_s)}{\sin \pi j}$$

$$- \pi\, \beta^{\pm}(s)\, [2\alpha^{\pm}(s)+1] \frac{P_{\alpha^{\pm}(s)}(-z_s)}{\sin \pi\, \alpha^{\pm}(s)}\,, \tag{I.4}$$

where the contours $C_{\pm}$ are shown in Fig. 8. Now $z_s = 1 + t/2q_s^2$, where q_s is related to s according to $s = 4(q_s^2 + m^2)$; hence, for large t,

$$a^{\pm}(j,s)\, P_j(-z_s) \approx [a^{\pm}(j,s)/(2q_s^2)^j]\, C(j)\, (-t)^j = b^{\pm}(j,s)\, C(j)\, (-t)^j\,,$$

where $C(j)$ is defined by

$$P_j(z) \xrightarrow[z \to \infty]{} C(j)\, z^j \,. \tag{I.5}$$

Thus from (I.2) and (I.4) it follows that the amplitude $A(s,z_s)$ will be asymptotic to an expression of the form

$$\begin{aligned} A(s,z_s) \approx\ & \frac{i}{4} \int_{C_+} dj(2j+1)\, b^+(j,s)\, C(j)\, \xi_+(j)\, \frac{t^j}{\sin \pi j} \\ & + \frac{i}{4} \int_{C_-} dj(2j+1)\, b^-(j,s)\, C(j)\, \xi_-(j)\, \frac{t^j}{\sin \pi j} \\ & + \sum_{\sigma = \pm} B^\sigma(s)\, \xi_\sigma(\alpha)\, \frac{t^{\alpha^\sigma(s)}}{\sin \pi\alpha^\sigma(s)} \,, \end{aligned} \tag{I.6}$$

where the signature factor $\xi_\pm(j)$ is defined by

$$\xi_\pm(j) = \exp(-i\pi j) \pm 1 \,. \tag{I.7}$$

Instead of $C_\pm$ we may, of course, choose any other contour which can be obtained by deforming $C_\pm$ in an arbitrary manner, as long as we avoid crossing any singularities. Since the real part of the position of the branch point is determined by a contour which minimizes the maximum of $\mathrm{Re}\, j$, where j is a point on that contour, we shall refer to it as the minimizing contour.

Finally we wish to briefly recapitulate the procedure followed by Amati, Fubini, and Stanghellini which led to the appearance of an angular momentum cut in the diagram of Fig. 3. As we have mentioned in

the introduction, AFS combined two Regge poles according to elastic unitarity in the t channel (see Fig. 3); thus for large t they approximated the absorptive part by

$$A_t(s,t) \approx \frac{B}{t} \int_{-\infty}^{0} ds' \int_{-\infty}^{0} ds'' \; R^*(t,s')\, R(t,s'')\, \tau(s,s',s'') \;, \quad (I.8)$$

where B is an overall constant, $A_t(s,t)$ is the t-channel absorptive part, and $R(t,s)$ stands for the amplitude associated with the exchange of a Regge pole; $\tau(s,s',s'')$ is the usual triangle function

$$\tau(s,s',s'') = \frac{\theta(-s^2-s'^2-s''^2+2ss'+2ss''+2s's'')}{\sqrt{-s^2-s'^2-s''^2+2ss'+2ss''+2s's''}} \;. \quad (I.9)$$

For $R(t,s)$, AFS chose the form

$$R(t,s) = C(s)\, \xi_+(\alpha)\, t^{\alpha(s)}/\sin \pi\alpha(s) \;, \quad (I.10)$$

where $\xi_\pm(\alpha)$ is given by (I.7). Substituting (I.10) into (I.8) one finds

$$A_t(s,t) \propto \int_{\ell_m}^{\ell_M} d\ell\, \rho(\ell,s)\, t^{\ell} \;, \quad (I.11)$$

where

$$\rho(\ell,s) = \int_{-\infty}^{0} ds' \int_{-\infty}^{0} ds'' \; \delta\big(\ell - \alpha(s') - \alpha(s'') + 1\big) \frac{C(s')}{\sin \pi\alpha(s')} \frac{C(s'')}{\sin \pi\alpha(s'')}$$

$$\times\; \xi_+^*\big(\alpha(s')\big)\, \xi_+\big(\alpha(s'')\big)\, \tau(s,s',s'') \;. \quad (I.12)$$

Formula (I.11) resembles the expression one would get from a continuous superposition of Regge poles; its asymptotic behaviour in t is determined by the upper integration limit, $\ell_M(s)$, where

$$\ell_M(s) = \max\,[\alpha(s') + \alpha(s'') - 1] ,$$

with s' and s'' within the domain of integration of (I.12). If $\alpha(s)$ is an increasing function of s for $s < 0$ (which is the case in their model), then $\alpha(s') + \alpha(s'') - 1$ takes on its maximum value on the boundary of the integration region (see Fig. 9). Using this fact one readily arrives at the inequality

$$\ell_M(0) \geqslant \ell_M(s) \geqslant \alpha(s) + \alpha(0) - 1 ;$$

the equality applies only for $s = 0$. The function $\alpha(s') + \alpha(s'') - 1$, with s' and s'' on the boundary of the integration region, has an extremum at $s' = s'' = s/4$; thus at this point: $\alpha(s') + \alpha(s'') - 1 \rightarrow 2\alpha(s/4) - 1$; we shall see in Section III that, for $s < 0$, the leading branch point in the angular momentum plane is, in fact, located at $2\alpha(s/4) - 1$ (this is not obvious since the above mentioned extremum could be a minimum).

II. THE SINGLE REGGE POLE EXCHANGE DIAGRAM

1. The AFS Approximation

In this section we analyze the diagram of Fig. 1 which in the elastic unitarity approximation gives rise to cuts in the angular momentum plane, in complete analogy to the results obtained in Section I. Rather than starting from the unitarity relation, as was done by Amati, Fubini, and Stanghellini,[1] and also by Mandelstam,[2] we shall follow Wilkin[4] in treating the diagram of Fig. 1 as a Feynman graph. Our methods will, however, be adapted to the specific purpose of exhibiting in as clear a way as possible the moving singularities in the angular momentum plane, and the mechanism which is responsible for their cancellation.

Consider then the Feynman amplitude corresponding to the diagram of Fig. 1:

$$A(s,t) = C \int dk_1^2\, dk_2^2\, dk_3^2\, dk_4^2\, J(k_n^2;s,t) \frac{1}{k_1^2 - m^2 + i\epsilon} \frac{1}{k_2^2 - m^2 + i\epsilon} \times \frac{1}{k_4^2 - m^2 + i\epsilon} R\left(\alpha(k_3^2),\ t; k_2^2, k_4^2\right), \tag{II.1}$$

where C is an overall constant, $J(k_n^2;\ s,t)$ is the Jacobian for the transformation

$$d^4k_1 \longrightarrow \prod_{n=1}^{4} dk_n^{\,2}$$

with the invariants s and t defined by $s = (q_1 - p_1)^2$ and $t = (p_1 + p_2)^2$ (see Fig. 1), and where $R\big(\alpha(k_3^2),\ t; k_2^2, k_4^2\big)$ is the amplitude associated with the exchange of a Regge pole with energy squared k_3^2, momentum transfer squared, $-t$, and variable external masses, k_2^2 and k_4^2; in practice one might take it to be of the form

$$R\big(\alpha(k_3^2),\ t; k_2^2, k_4^2\big) = \beta(k_3^2; k_2^2, k_4^2)\ \frac{C(\alpha)}{\sin \pi\alpha(k_3^2)}\ (-\cos\theta_3)^{\alpha(k_3^2)}. \quad \text{(II.2)}$$

Here $\beta(k_3^2;\ k_2^2,\ k_4^2)$ is the residue of the Regge pole, $C(\alpha)$ is the coefficient in the asymptotic expansion of the Legendre function [i.e., $P_\alpha(z) \longrightarrow C(\alpha)\ z^\alpha$], and $\cos\theta_3$ is the c.m. scattering angle in the channel where k_3^2 is the square of the c.m. energy; in terms of the invariants it is given by

$$\cos\theta_3 = \frac{2k_3^2(t - 2m^2) + (k_3^2 + m^2 - k_2^2)(k_3^2 + m^2 - k_4^2)}{\sqrt{(k_3^2 + m^2 - k_2^2)^2 - 4m^2k_3^2}\ \sqrt{(k_3^2 + m^2 - k_4^2)^2 - 4m^2k_3^2}}\ . \quad \text{(II.3)}$$

As we shall see later, we do not require an explicit expression for the Regge pole in order to prove the cancellation of the AFS cut; only its general properties are needed. This is fortunate, since in writing down (II.2), or similar expressions, we will, in general, have mutilated the analytic structure of the original Feynman amplitude associated with the exchange of a Regge pole.

Now the Jacobian, $J(k_n^2;\ s,t)$, is given (we suppress the arguments) by the following expression

$$J = \Theta(D)/\sqrt{D} \quad , \tag{II.4}$$

where

$$D = -16 \operatorname{Det}|2k_i \cdot k_j|$$

$$= -16 \begin{vmatrix} 2k_1^2 & k_1^2+k_2^2-m^2 & k_1^2+k_3^2-s & k_1^2+k_4^2-m^2 \\ k_1^2+k_2^2-m^2 & 2k_2^2 & k_2^2+k_3^2-m^2 & k_2^2+k_4^2-t \\ k_1^2+k_3^2-s & k_2^2+k_3^2-m^2 & 2k_3^2 & k_3^2+k_4^2-m^2 \\ k_1^2+k_4^2-m^2 & k_2^2+k_4^2-t & k_3^2+k_4^2-m^2 & 2k_4^2 \end{vmatrix} .$$

Evaluation of the determinant yields, for $s/t \ll 1$, and $m^2/t \ll 1$,

$$D = 16\, t^2 \left\{ 4sk_3^2 - (k_1^2 - s - k_3^2)^2 + 4\left(\frac{s}{t}\right) \left[(k_3^2 + m^2 - k_2^2)\,(k_3^2 + m^2 - k_4^2) \right.\right. \tag{II.5}$$

$$\left.\left. + (k_1^2 - s - k_3^2)(k_3^2 + m^2 - \tfrac{1}{2} k_2^2 - \tfrac{1}{2} k_4^2) + \frac{s-8m^2}{4t} (k_2^2 - k_4^2)^2 \right] \right\} .$$

Now we are interested only in the leading contribution to (II.1) for $t \to \infty$; we therefore may approximate the right-hand side of (II.5) by the first two terms, since the remainder becomes comparable in magnitude only when k_2^2 or k_4^2 (or both) become of the order of t, in which case the contribution to the integral is already damped by a factor of

$1/t$ due to the presence of the Feynman propagators involving k_2^2 and k_4^2. Hence for large t we obtain as our leading contribution to the amplitude (II.1)

$$[A(s,t)]_{l.c.} = \frac{C}{4t} \int dk_1^2 \; dk_3^2 \; \tau(k_1^2, k_3^2, s) \; \frac{1}{k_1^2 - m^2 + i\epsilon}$$
$$\times \int dk_2^2 \, dk_4^2 \; \frac{1}{[k_2^2 - m^2 + i\epsilon][k_4^2 - m^2 + i\epsilon]} \; R\big(\alpha(k_3^2),\; t; k_2^2, k_4^2\big), \tag{II.6}$$

where $\tau(k_1^2, k_3^2, s)$ is the triangle function defined by (I.9). From the present point of view the AFS approximation corresponds to ignoring the singularities of $R\big(\alpha(k_3^2),\; t; k_2^2, k_4^2\big)$ in k_2^2 and k_4^2. Now, for k_2^2 fixed at a finite value, $R \approx 1/k_2^2$ as $k_2^2 \to \infty$;[11] we may therefore close the k_2^2 integration contour in the lower half of the complex plane, and hence pick up the contribution from the pole of the propagator (recall that we are ignoring the singularities of R). Repeating the same procedure with the k_4^2 integration, we obtain the following expression for the AFS amplitude:[12]

$$[A(s,t)]_{AFS} = -\pi^2 \; \frac{C}{t} \int dk_3^2 \; R\big(\alpha(k_3^2), t\big) \int dk_1^2 \; \frac{\tau(k_1^2, k_3^2, s)}{k_1^2 - m^2 + i\epsilon} \;, \tag{II.7}$$

where $R\big(\alpha(k_3^2), t\big) \equiv R\big(\alpha(k_3^2), t; m^2, m^2\big)$. At this point we could perform immediately the k_1^2 integration; however, it turns out to be convenient to leave it in the form (II.7).

2. Representation of the AFS Amplitude as a Contour Integral in the Energy Plane of the Exchanged Regge Pole

Consider expression (II.7) with[13]

$$R\big(\alpha(k_3^2),t\big) = \gamma(k_3^2)\, C(\alpha)\, \xi(\alpha)\, t^{\alpha(k_3^2)}/\sin \pi\alpha(k_3^2)\ , \tag{II.8}$$

where $\gamma(k_3^2)$ is related to the full residue $\beta(k_3^2)$ appearing in (I.4) by

$$\gamma(k_3^2) = -\frac{\pi}{2}\,(2\alpha + 1)\,\beta(k_3^2)/(2q^2)^{\alpha}\ . \tag{II.9}$$

Here $q^2 = -m^2 + k_3^2/4$. It turns out convenient to change the integration variables in (II.7) from k_3^2 and k_1^2, to x and k_z, where[14]

$$x = k_3^2 - (1/4s)\,(k_1^2 - s - k_3^2)^2$$

and

$$k_z = (k_1^2 - s - k_3^2)/2\sqrt{-s}\ .$$

We then obtain, for the AFS amplitude valid for $s < 0$,

$$[A(s,t)]_{AFS} = -\pi^2 C \int_{-\infty}^{0} \frac{dx}{\sqrt{-x}} \int_{-\infty}^{+\infty} dk_z \frac{\gamma(x - k_z^2)}{x - (k_z - \sqrt{-s})^2 - m^2} \times C(\alpha)\,\xi(\alpha)\, \frac{t^{\alpha(x - k_z^2) - 1}}{\sin \pi\alpha(x - k_z^2)} \tag{II.10}$$

Consider for a moment the integrand of the k_z integration; it is singular at (the positions of the singularities are shown in Fig. 10a)

$$k_z = \sqrt{-s} \pm i\sqrt{m^2 - x} \qquad \text{(II.11a)}$$

and also at

$$k_z = \pm i\sqrt{u_n - x} \quad , \qquad \text{(II.11b)}$$

where the latter singularities arise from the normal threshold branch points of the Regge trajectory, $\alpha(k_3^2)$, and residue, $\gamma(k_3^2)$, and from the vanishing of $\sin \pi\alpha(k_3^2)$ at the bound states and resonances which lie on the trajectory; u_n stands for the various values of k_3^2 at these singularities. The above k_z-integration contour may, of course, be deformed in an arbitrary manner, as long as we stay away from any singularities. So far the integral (II.10) is only valid, as it stands, for $s < 0$. In continuing it to positive s, we must make sure that at no stage in the continuation the above singularities will cross the integration contours. As we increase s through negative values, the complex singularities (II.11a) will move towards the imaginary axis, which they reach for $s = 0$. For $s > 0$ the singularities remain on the imaginary axis, <u>both</u> moving either up or down depending on the continuation chosen for the function $\sqrt{-s}$ (i.e., down : $\sqrt{-s} = -i\sqrt{s}$, and up : $\sqrt{-s} = i\sqrt{s}$). As s becomes larger than $m^2 - x$, one of the singularities will cross the real k_z axis,

and drag the integration contour along the imaginary axis, as is shown in Figs. 10b and 10c (we have displaced the k_z-integration contour slightly into the upper half plane to facilitate the subsequent discussion of the integral (II.10); we could, of course, have just as well displaced it into the lower half plane). We now make a final change of variables from k_z and x, to $u = x - k_z^2$ and x. The above discussion in the k_z plane was only intended to serve as a crutch for a better understanding of the analysis that follows, as well as of the similarity existing between the single and double Regge pole exchange diagrams. With the above change of variables, (II.10) becomes[15]

$$[A(s,t)]_{AFS} = \frac{i}{2} \int_{C_u} du\, c(u,s)\, \frac{t^{\alpha(u)-1}}{\sin \pi\alpha(u)} \left(e^{-i\pi\alpha(u)} \pm 1\right), \qquad \text{(II.12a)}$$

where

$$c(u,s) = -i\pi^2 C\, \gamma(u)\, C(\alpha)\, I(u,s) \qquad \text{(II.12b)}$$

and

$$I(u,s) = \int_{-\infty}^{0} \frac{dx}{\sqrt{-x}\,\sqrt{x-u}} \; \frac{1}{u + s - m^2 + 2\sqrt{-s}\,\sqrt{x-u}}\,. \qquad \text{(II.12c)}$$

The contour C_u is shown in Fig. 11. If we define $\ell = \alpha(u) - 1$, then (II.12a) can also be written as

$$[A(s,t)]_{AFS} = \frac{i}{2} \int_{C_\ell} d\ell\, (2\ell + 1)\, \tilde{c}(\ell,s)\, \frac{t^{\ell}}{\sin \pi\ell} \left(e^{-i\pi\ell} \mp 1\right), \qquad \text{(II.13)}$$

where $\tilde{c}(\ell,s) = c(\lambda(\ell),s)/(2\ell+1)\alpha'$; here $\lambda(\ell)$ is the inverse of the transformation $\ell = \alpha(u) - 1$, and α' is the derivative of $\alpha(u)$. The contour C_ℓ shown in Fig. 12a has been obtained using the fact that $\alpha(u)$ is a real analytic function of u with the usual right-hand cut beginning at the lowest threshold. From here it follows that as long as the contour C_u does not cross this cut, complex conjugate points in the u plane will map into complex conjugate points in the ℓ plane; assuming that $\alpha(u)$ satisfies a dispersion relation with at most one subtraction (which is very reasonable), one can verify that for $u < 0$, it is an increasing function of that variable; we thus arrive at the contour C_ℓ shown in Fig. 12a. We wish to remark at this point that the quantity ℓ in (II.13) is not to be identified with the complex angular momentum j appearing in (I.6). In fact, $\ell \equiv \alpha - 1$ can be regarded as the total angular momentum in the s channel obtained by coupling the (variable) "spin" α of the Regge pole to a relative orbital angular momentum L, where $L = -1$. If the Regge pole in (II.7) were replaced by an elementary particle of spin σ, then the partial-wave amplitude would have a singularity at $j = \sigma - 1$; in fact, this singularity would also be present in the full amplitude (II.1).[16] The Reggeization of the particle results in the replacement of σ by $\alpha(u)$, and the branch points of $[A(s,t)]_{AFS}$ in the angular momentum plane can be looked upon as arising from an extension of this singularity throughout the Regge trajectory.

3. Location of the Singularities in the j plane

Let us return to expression (II.12c) and rewrite it as follows:

$$I(u,s) = \frac{1}{4s} \int_{-\infty}^{0} \frac{dx}{\sqrt{-x}\,\sqrt{x-u}} \; \frac{R(u,s,x)}{x - x_P(s,u)} , \qquad \text{(II.14a)}$$

where

$$R(u,s,x) = u + s - m^2 - 2\sqrt{-s}\,\sqrt{x-u} \qquad \text{(II.14b)}$$

and

$$x_P(u,s) = (-1/4s)\,[(u + s - m^2)^2 - 4\,su]$$

$$= (-1/4s)\,[u - (m + i\sqrt{-s})^2]\,[u - (m - i\sqrt{-s})^2] . \qquad \text{(II.14c)}$$

The integrand of (II.14a) is singular at

$$\begin{aligned} &\text{(a)} \quad x = 0 , \\ &\text{(b)} \quad x = u , \\ &\text{(c)} \quad x = x_P(u,s) , \end{aligned} \qquad \text{(II.15a)}$$

with the possible exception of (c), since the residue function $R(u,s,x)$ might vanish at the pole. The singularities of $I(u,s)$ will then be generated by the collision of the moving singularities (b) and (c) with the end point of the integration contour, or, by the pinching of the

contour due to (a) and (c) [any pinches that arise from the collisions of (b) and (c) are expected to give rise to regular points of $I(u,s)$, since the residue $R(u,s,x)$ vanishes at the pinch]. We conclude that $I(u,s)$ will be singular at

$$\text{(d)} \quad u = 0$$

and possibly at (II.15b)

$$\text{(e)} \quad u = (m \pm i\sqrt{-s})^2 \equiv u_{\pm} \quad ,$$

where we say "possibly," since the singularity might be absent due to the vanishing of the residue function (II.14b) at the pole. The analytic properties of $I(u,s)$ on the various sheets associated with the branch point at $u = 0$ may be obtained directly from the integral representation (II.14a). In Figs. 13a through 18a we have shown several paths of continuation in the u plane, all of which start from a given point u_0 just above the negative u axis and lead to the point $u = u_{\pm}$. The new contours of integration which emerge from the continuations are shown in Figs. 13b(c) through 18b(c); the motion of the pole at $x' = x_P$ is shown by the dashed lines; to keep the picture as clear as possible we have not shown the corresponding paths taken by the square root singularity at $x = u$. As we have already mentioned, the presence or absence of the singularities at $u = u_+$ and $u = u_-$ is determined by the behaviour of $R(u_{\pm},s,x)$ at the end point of the integration contour, or, at the pinch arising from the coincidence of (a) and (c) in (II.15a). We shall illustrate the method used for establishing the analytic properties of $I(u,s)$ at $u = u_{\pm}$ with a few examples.[17]

We shall take the point $u = u_0$ to lie on the contour C_u of (II.12a). Retracing our steps which led from formula (II.10) to (II.14a) then shows that we must choose the branch of the square root, $\sqrt{x - u}$, for which

$$\sqrt{x - u_0} = + i \left|\sqrt{x - u_0}\right| ; \quad \text{if} \quad x - u_0 < 0 . \tag{II.16}$$

Let us fix x at some point on the contour C_x which remains unaffected by the continuation of $I(u,s)$ in u along the various paths shown in Figs. 13a through 18a; call this point, $x = x_C$. We then obtain from (II.16) that

$$R(u_\pm, s, x_C) = u_\pm + s - m^2 - 2\sqrt{-s}\,\sqrt{x_C - u_\pm} , \tag{II.17a}$$

where $\sqrt{x_C - u_\pm}$ has a <u>nonnegative</u> imaginary part. Since

$$\left|u_\pm + s - m^2\right| = \left|2\sqrt{-s}\,\sqrt{-u_\pm}\right| \tag{II.17b}$$

it follows that the vanishing of $R(u_\pm, s, x)$ at $x = 0$ will depend only on the phase of $\sqrt{x - u_\pm}$ at that point; we obtain this phase by continuing (II.17a) in x_C along the integration contour C_x. A brief reflection shows that unless C_x crosses the right-hand cut of the square root function associated with the branch point at $x = u_\pm$, $\sqrt{x - u_\pm}$ will be always of the form $a + ib^2$ everywhere along the contour, where a and b are real quantities. Such is

the case, for example, for the continuations shown in Figs. 13b and 14b. Since $\mathrm{Im}\sqrt{-u_\pm} > 0$, we conclude from (II.17a,b) that the residue function vanishes at the end-point of the integration contour for $u = u_+$, but not for $u = u_-$. Hence $I(u,s)$ is found to be singular at $u = u_-$, but regular at $u = u_+$. To find the singularities of $I(u,s)$ on the sheets reached by continuing this function either clockwise or counterclockwise around the branch point at $u = 0$, we must continue (II.17a) in x_C along the contours shown in Figs. 15 through 18. As an example we consider the clockwise continuation to the point $u = u_-$ (see Fig. 15a,b,c). Since the contour C_x crosses the right-hand cut of $\sqrt{x - u_-}$, the residue function will now vanish at the end-point of the integration contour. Nevertheless, $I(u,s)$ is still singular at $u = u_-$ due to a pinching of the contour by the pole at $x = x_P$, and the fixed singularity at $x = 0$ (notice that the residue function does <u>not</u> vanish at the pinch!). A similar analysis can be carried out for the paths of continuation shown in Figs. 16 through 18. The conclusion reached is that $I(u,s)$ is regular at $u = u_+$ on the "leading" sheet,[18] but singular on the remaining sheets, while it is regular at $u = u_-$ on the sheet reached by a counterclockwise continuation around the branch point at $u = 0$, but singular on the other two (actually there are an infinite number of these sheets, of which we have analyzed only the nearest neighbours of the leading one). The situation for $s > 0$ is depicted in Figs. 19 through 24, where, once again, we have shown the various paths of continuation in the u plane, together with the integration contours that result from the continuation; as before, the

corresponding paths followed by the pole at $x = x_p$ are indicated by the dashed curves. The analysis of the various continuations proceeds along the same lines as before; the main differences with the previous case being that: (1) the singularities at $u = u_\pm$ have moved onto the real axis, and now appear at $u_\pm = (\sqrt{s} \pm m)^2$, and (2) we must distinguish among the two possible continuations of the function $\sqrt{-s}$ around the branch point at $s = 0$ (i.e. $\sqrt{-s} = \pm i\sqrt{s}$, $s > 0$); thus for $s > 0$, (II.17a) becomes:

$$R(u_\pm, s, x_c) = u_\pm + s - m^2 - 2(\pm i\sqrt{s})\sqrt{x_c - u_\pm} \quad .$$

It is clear that as long as the singularities at $u = (\sqrt{s} \pm m)^2$ [on whatever sheet of $I(u,s)$ they might appear] do not cross the left-hand cut of $I(u,s)$ arising from the branch point at $u = 0$, they cannot leave their respective sheets. Hence, for $s < m^2$, we must reach the <u>same</u> conclusions as before with regard to the singularity structure of $I(u,s)$ at $u = (\sqrt{s} + m)^2$ and $u = (\sqrt{s} - m)^2$, where these points are analytic continuations of $u = (m \pm i\sqrt{-s})^2$ in s to $0 < s < m^2$. Thus, for example, if we chose the continuation, $\sqrt{-s} = +i\sqrt{s}$, then all our previous findings about the points $u = (m + i\sqrt{-s})^2$ and $u = (m - i\sqrt{-s})^2$ will now apply to their respective continuations, i.e., $u = (\sqrt{s} - m)^2$, and $u = (\sqrt{s} + m)^2$. The analysis of Figs. 19 through 24 shows that this is indeed the case. For $s > m^2$, the singularity of $I(u,s)$ at $u = (\sqrt{s} - m)^2$ has moved onto a different sheet of the branch point at $u = 0$; if it was absent on the

"leading" sheet for $0 < s < m^2$ (which is the case if we take $\sqrt{-s} = i\sqrt{s}$) it will now be present for $s > m^2$, but absent from the sheet reached by a counterclockwise continuation of $I(u,s)$ around $u = 0$; alternatively, if it was present for $0 < s < m^2$, it will now be absent from the leading sheet, but present on the other two reached by a clockwise or counterclockwise continuation.

The above conclusions may be easily translated into the complex ℓ plane, where $\ell = \alpha(u) - 1$. From the structure of (II.12b) it is evident that the singularities of $c(u,s)$ which arise from those of $I(u,s)$ appear on all the sheets of $\alpha(u)$ and $\gamma(u)$ associated with the normal threshold branch points; if we denote the value of $\alpha(u)$ on the i'th sheet by $\alpha^i(u)$, then we conclude from the above discussion in the u plane that $\tilde{c}(\ell,s)$ will have singularities at $\ell = \alpha^i(0) - 1$ and $\ell = \alpha^i\left((m \pm i\sqrt{-s})^2\right) - 1$, where the latter ones appear on all sheets of the former with the exception of a single one. Let $\ell = \alpha^1(0) - 1$ be the singularity enclosed by the contour C_ℓ in (II.13); it then follows from the analytic structure of $I(u,s)$ in u, that as we increase s above m^2 a new singularity located at $\ell = \alpha^1\left((\sqrt{s} - m)^2\right) - 1$ will appear on the leading sheet of $\tilde{c}(\ell,s)$ via the branching at $\ell = \alpha^1(0)-1$; thus the new contour in the ℓ plane will appear as shown in Fig. 12b [in the above discussion we considered the continuation of $\sqrt{-s}$ to $s > 0$ according to a $-i\epsilon$ prescription; it is clear, however, that our conclusions do not depend on the choice for this continuation, since we could have just as well displaced the k_z-integration contour of (II.10) into the lower half plane, in which case a $+i\epsilon$ prescription would lead to the same situation described above]. The general situation in the

ℓ plane can be illustrated with a simple example: let $\alpha(u) = \frac{1}{2}(3 - \sqrt{4 - u})$, where the u plane is cut from threshold (that is, $u = 4$, in units of m^2) along the positive axis. One then arrives in a straightforward manner at the picture shown in Fig. 25, where "I" and "II" label the regions of the complex ℓ plane that are mapped onto the first and second sheets of $\alpha(u)$. All the singularities of $I(u,s)$ will in turn be imaged into a corresponding set appearing in each of these regions, and their associated sheet structure will be the same as that we have found above [in general there will of course exist additional singularities arising from the transformation, $\ell = \alpha(u)-1$]. From the above discussion we conclude that, except for logarithmic factors, the asymptotic behaviour in t of the AFS amplitude is given by

$$[A(s,t)]_{AFS} \approx \begin{cases} t^{\alpha(0)-1} & ; \quad s \leqslant m^2 \\ t^{\alpha\left((\sqrt{s}-m)^2\right)-1} & ; \quad s \geqslant m^2 \end{cases} .$$

This result is in agreement with the findings of Mandelstam[2] and Wilkin[4] [the asymptotic form $t^{\alpha(0)-1}$ for $s < m^2$ was found originally by Wilkin]. The precise form for the asymptotic behaviour of the AFS amplitude can be obtained directly from (II.10) for $s < m^2$ and its continued form for $s > m^2$, or, from the expression (II.12) if the discontinuity of $c(u,s)$ is known; since we shall anyway obtain the formula for the discontinuity in the following section, it is easiest to take the latter approach.

4. Formulae for the Discontinuities of $c(u,s)$, and Asymptotic Behaviour of the AFS Amplitude

Having found the location of the singularities of $c(u,s)$ in the complex u plane, we now wish to obtain explicit formulae for the discontinuities across the various cuts. Whereas the positions of the singularities are the same for the more complicated diagrams which do exhibit angular momentum cuts (as we shall see in Section IV), one would not expect that the strength of the discontinuities will be the same. In Section IV, however, we shall see that in a certain approximation the discontinuity functions for the diagrams of Figs. 1 and 2, and Figs. 3 and 4 are, in fact, proportional to each other, the proportionality factor being the square of an integral over the amplitude associated with the "cross" in Figs. 2 and 4. Since in the following section we shall obtain an explicit expression for the function $c(u,s)$ defined in (II.12a), the present discussion might appear redundant. However, since the formulae for the discontinuities can be obtained in a straightforward way, whereas it takes a fair amount of effort to unscramble the various sheets of $c(u,s)$, we shall proceed to evaluate the discontinuities and use them as a check on the function $c(u,s)$ to be obtained subsequently.

Let us then consider the integral (II.7) which, as it stands, is valid only for $s < 0$. Upon performing the integration over k_1^2, we find

$$[A(s,t)]_{AFS} = \pi^3 C \int_{-\infty}^{0} \frac{du}{\sqrt{(u+s-m^2)^2-4su}} \frac{\gamma(u)}{\sin \pi\alpha(u)} C(\alpha)\xi(\alpha)\, t^{\alpha(u)-1} . \tag{II.18}$$

Aside from the singularities arising from the normal threshold branch points of $\alpha(u)$ and $\gamma(u)$, the integrand of (II.18) is singular at $u = s + m^2 \pm 2\, im\sqrt{-s}$. Notice that the fixed singularity at $u = 0$ [or equivalently, at $\ell = \alpha(0) - 1$], found in the previous section, does not appear in (II.18). This is an indication that we are dealing with a logarithmic branch point at $u = 0$, in agreement with the result to be obtained in the following section. Comparison of (II.12) and (II.18) shows that the latter integral involves an integration over the discontinuity in u of $c(u,s)$. We now continue formula (II.18) to $s > 0$; as before we must make sure that at no stage in the continuation the singularities at $u = s + m^2 \pm 2\, im\sqrt{-s}$ cross the integration contour. Now as s approaches zero these singularities move towards the real axis along complex conjugate paths. Independent of the particular continuation chosen for the function $\sqrt{-s}$, one of these singularities will approach $u = 0$ along the positive axis, while the other keeps receding towards the right and hence will never meet the contour of integration. Thus, as $s \to m^2$, the singularity at $u = (\sqrt{s} - m)^2$ will catch the integration contour of (II.18) and will pull it to the right as we keep increasing s above m^2; for $s > m^2$ the new contour will therefore appear as shown by the solid or dashed lines in Figs. 26a,b, depending on whether the path of continuation in the s plane passes below or above the point $s = m^2$. We thus arrive at the following expression for the continued AFS amplitude, which is the same for both of the above mentioned paths of continuation [this is not surprising since one can verify that the integral (II.18) is not singular at $s = m^2$]:

$$[A(s,t)]_{AFS} = \pi^3 C \int_{-\infty}^{0} \frac{du}{\sqrt{(u+s-m^2)^2-4su}} \frac{\gamma(u)}{\sin \pi\alpha(u)} C(\alpha)\, \xi(\alpha)\, t^{\alpha(u)-1}$$

$$+ 2\pi^3 C \int_{0}^{(\sqrt{s}-m)^2} \frac{du}{\sqrt{(u+s-m^2)^2-4su}} \frac{\gamma(u)}{\sin\pi\alpha(u)} C(\alpha)\xi(\alpha)\, t^{\alpha(u)-1}, \tag{II.19}$$

where $C(\alpha)$ and $\xi(\alpha)$ are defined by (I.5) and (I.7) with $j \to \alpha$. Comparing (II.19) with (II.12a), we see that

$$\mathrm{disc}_u\ c(u,s) = \begin{cases} \dfrac{-2i\pi^3 C}{\sqrt{(u+s-m^2)^2-4su}}\ \gamma(u)\, C(\alpha), & \text{for } u < 0, \qquad \text{(II.20a)} \\[2ex] \dfrac{-4i\pi^3 C}{\sqrt{(u+s-m^2)^2-4su}}\ \gamma(u) C(\alpha)\theta(s-m^2), & \text{for } u > 0. \qquad \text{(II.20b)} \end{cases}$$

The above formulae will serve as a check on the function $c(u,s)$ to be obtained in the following section.

The asymptotic behaviour of the AFS amplitude may now be obtained immediately from the expression (II.19); thus for s strictly less than m^2 the integrand is seen to approach a constant as $u \to 0$. Now for $t \to \infty$ the leading contribution to the amplitude comes from the integration region near $u = 0$. Let us therefore expand $\alpha(u)$ around $u = 0$, keeping only the linear terms; we then obtain

$$[A(s,t)]_{AFS} = \pi^3 C \left(\frac{\gamma(0)}{\sin \pi\alpha} \frac{1}{m^2 - s} C(\alpha)\, \xi(\alpha)\right) t^{\alpha(0)-1} \int_{-\epsilon}^{0} du\, t^{\alpha'(0)u}$$

$$+ O\left(t^{\alpha(0)-1-\alpha'(0)\epsilon}\right); \quad \alpha \equiv \alpha(0) .$$

Hence, for $s < m^2$,

$$[A(s,t)]_{AFS} \approx \pi^3 C \left(\frac{\gamma(0)}{\sin \pi\alpha} \frac{1}{m^2 - s} C(\alpha)\, \xi(\alpha)\right) \frac{t^{\alpha(0)-1}}{\alpha' \ln t} ,$$

$$\alpha \equiv \alpha(0), \ \alpha' \equiv \alpha'(0) . \qquad \text{(II.21)}$$

The asymptotic behaviour of the amplitude for $s > m^2$, on the other hand, is determined by the second integral in (II.19); its integrand is seen to diverge as $u \to (\sqrt{s} - m)^2$. Proceeding in an analogous manner as above, we find

$$[A(s,t)]_{AFS} \approx 2\pi^3 C \left(\frac{\gamma(u_-)}{\sin \pi\alpha} \frac{1}{(4m\sqrt{s})^{\frac{1}{2}}} C(\alpha)\, \xi(\alpha)\right) t^{\alpha-1} \int_{u_- -\epsilon}^{u_-} \frac{du}{\sqrt{u_- - u}}\, t^{\alpha'[u-u_-]},$$

$$\alpha \equiv \alpha(u_-), \ \alpha' \equiv \alpha'(u_-) ,$$

where $u_- = (\sqrt{s} - m)^2$. Making a change of integration variables, we obtain

$$[A(s,t)]_{AFS} \approx 2\sqrt{\pi}\, \pi^3 C \left(\frac{\gamma(u_-)}{\sin \pi\alpha} \frac{C(\alpha)\xi(\alpha)}{(4m\sqrt{s})^{\frac{1}{2}}}\right) \frac{t^{\alpha-1}}{\sqrt{\alpha' \ln t}} \operatorname{erf}(\sqrt{\alpha'\epsilon \ln t}),$$

$$\alpha \equiv \alpha(u_-), \ \alpha' \equiv \alpha'(u_-) , \qquad \text{(II.22)}$$

where $\mathrm{erf}(x)$ is the well-known error function

$$\mathrm{erf}(x) = \frac{2}{\sqrt{\pi}} \int_0^x dt\, e^{-t^2} \underset{x\to\infty}{\approx} 1 - \frac{e^{-x^2}}{x\sqrt{\pi}} \left(1 - 2!/(2x)^2 + \cdots\right). \quad \text{(II.23)}$$

From (II.22) and (II.23) we therefore find that

$$[A(s,t)]_{AFS} \approx G(s)\; t^{\alpha\left((\sqrt{s}-m)^2\right)-1}/(\ell n\, t)^{\frac{1}{2}}, \text{for } s > m^2 , \quad \text{(II.24a)}$$

where

$$G(s) = \sqrt{\pi}\; \pi^3 C \left(\frac{\gamma(u_-)}{\sin \pi\alpha} \; \frac{C(\alpha)\; \xi(\alpha)}{(m\, \alpha'\sqrt{s})^{\frac{1}{2}}}\right) ,$$

with

$$\alpha \equiv \alpha(u_-),\; \alpha' \equiv \alpha'(u_-) \quad \text{(II.24b)}$$

and

$$u_- = (\sqrt{s} - m)^2 .$$

If the AFS amplitude has a Sommerfeld-Watson representation [i.e., it can be written in the form (I.6)], then we conclude from the asymptotic behaviour (II.21) and (II.24) that the analytically continued partial-wave amplitude associated with the s reaction must have a logarithmic singularity at $j = \alpha(0) - 1$, and an additional singularity at $j = \alpha\left((\sqrt{s} - m)^2\right) - 1$, for $s > m^2$, which is of the inverse square-root type.

5. Evaluation of $c(u,s)$

We now wish to obtain an explicit expression for the function $c(u,s)$ defined by (II.12b,c). Although we do not expect its detailed structure to be that of the corresponding function for the more complicated diagrams which do exhibit angular momentum cuts (see Fig. 2, for example), we nevertheless believe that the nature of the singularities will probably remain the same. It is the purpose of this section to investigate the types of branch points of $c(u,s)$ that we are dealing with, and also to confirm, and complete, our analysis of the sheet structure of this function which we began in Section 3. In addition we shall verify the formulae for the discontinuities obtained in the previous section. Consider then the integral (II.12c),

$$I(u,s) = \int_{-\infty}^{0} \frac{dx}{\sqrt{-x}\,\sqrt{x-u}} \; \frac{1}{u+s-m^2+2\sqrt{-s}\,\sqrt{x-u}} \,. \qquad \text{(II.25)}$$

Here s is to be taken negative. A closer examination of (II.25) shows that it is easiest to evaluate it for u fixed within the domain $0 < u < m^2 - s$, for any phase ambiguities can then be readily removed; this will become clear below. Since for $s < 0$ the singularity at $x = (-1/4s)\,[(u+s-m^2)^2 - 4su]$ of the integrand (a pole) lies on the positive real axis for all real values of u, it is immaterial whether we evaluate (II.25) for $u < 0$ or $u > 0$, for the two expressions so obtained are analytic continuations of each other. We therefore shall evaluate (II.25) with u fixed at a point located on the sheet on which the contour C_u is exposed [see formula

(II.12a) and also Fig. 11], and lying within the above-mentioned range. As we have already remarked in Section 3, the above choice for u implies that we must take the branch of $\sqrt{x - u}$ given by (II.16). Let

$$g(u,s) = (1/4s)[(u + s - m^2)^2 - 4su] .$$

The integral (II.25) may be split up as follows

$$I(u,s) = I_1(u,s) + I_2(u,s) ,$$

where

$$I_1(u,s) = \frac{u + s - m^2}{4is} \int_{-\infty}^{0} \frac{dx}{\sqrt{-x}\,\sqrt{u - x}} \frac{1}{x + g(u,s)}$$

and

$$I_2(u,s) = - \frac{\sqrt{-s}}{2s} \int_{-\infty}^{0} \frac{dx}{\sqrt{-x}} \frac{1}{x + g(s,u)} .$$

Throughout this paper we shall adopt the conventions that: (a) <u>all square roots are to be taken positive if their discriminant is positive, and</u> (b) <u>$\ell n\, z$ is to be taken real for $z > 0$.</u> Notice that for $0 < u < m^2 - s$ the phases of I_1 and I_2 are given by $I_1 = + ic^2$, and $I_2 = - b^2$, where c^2 and b^2 are positive quantities. The above integrals for I_1 and I_2 may be performed with the use of standard tables; we find that

$$I(u,s) = \frac{\pi}{\sqrt{K(u,s,m^2)}} \left[-1 + i(2/\pi)\, \ell n\left(\frac{\sqrt{K(u,s,m^2)} - (u+s-m^2)}{2\sqrt{-s}\,\sqrt{u}} \right) \right], \quad \text{(II.26a)}$$

where

$$\begin{aligned} K(u,s,m^2) &= u^2 + s^2 + m^4 - 2us - 2um^2 - 2sm^2 \\ &= (u+s-m^2)^2 - 4su \ . \end{aligned} \quad \text{(II.26b)}$$

An alternative form for (II.26a) which we shall find very convenient is

$$I(u,s) = \frac{i}{\sqrt{K(u,s,m^2)}}\, \ell n\left(\frac{\sqrt{K(u,s,m^2)} - (u+s-m^2)}{\sqrt{K(u,s,m^2)} + (u+s-m^2)} \right) \exp(i\pi) \ . \quad \text{(II.26c)}$$

<u>a. $s < 0$</u>

For $s < 0$ and u an arbitrary positive number, the phase of the quantity in brackets appearing in the argument of the logarithm in (II.26a) or (II.26c) is chosen to be zero. $I(u,s)$ can then be continued to all complex s and u. From (II.26a) or (II.26c) we see that the possible singular points of $I(u,s)$ in u are located at

(1) $u = (m \pm i\sqrt{-s})^2 \equiv u_{\pm}$,

(2) $u = 0$,

where, for $s < 0$, the latter singularity arises from the vanishing of the denominator in the argument of the log. If we cut the u plane from $u = 0$ along the negative real axis, then the contour C_u of the integral (II.12a) extends around this cut, and the value of $I(u,s)$ on that contour is obtained by continuing (II.26a) or (II.26c) in u to the points $u_0 \pm i\epsilon$, where $u_0 < 0$; from here on we shall refer to the sheet of the logarithmic branch point at $u = 0$ which contains the contour C_u as the "leading sheet." We now wish to verify that $I(u,s)$ is singular at $u = u_-$, where this point is reached by the path shown in Fig. 13a, and regular at $u = u_+$ if this point is reached by the corresponding path shown in Fig. 14a. Let

$$z = \frac{\sqrt{K(u,s,m^2)} - (u + s - m^2)}{\sqrt{K(u,s,m^2)} + (u + s - m^2)} \quad . \tag{II.27}$$

Recalling that the phase of z is taken to be zero for $s < 0$ and $u > 0$, one may readily verify that

$$z \to \exp(\mp i\pi), \text{ as } u \to u_\pm \quad .$$

By carefully following the phase of z as we take u around the points $u = u_+$ and $u = u_-$, one finds that

$$[\Delta_u I(u,s)]_{u_-} = -4\pi/[K(u,s,m^2)]^{\frac{1}{2}}$$

and

$$[\Delta_u I(u,s)]_{u_+} = 0 \ .$$

We conclude that $I(u,s)$ is regular at $u = u_+$, and singular at $u = u_-$, where these points are reached via the paths shown in Figs. 13a and 14a. To establish the singularity structure of $I(u,s)$ on the remaining sheets of the logarithmic branch point, we start from formula (II.26c) and continue it in u from the positive axis clockwise, or counterclockwise around the singularity at $u = 0$; this gives rise to a phase for z equal to $\exp(2in\pi)$ or $\exp(-2in\pi)$ respectively, where n is the number of times we encircle the origin [this result is even more evident from the form (II.26a)]; proceeding as before, we find that $I(u,s)$ is regular at $u = u_-$, where this point is reached by a counterclockwise continuation once around $u = 0$, and singular on all the remaining sheets of the logarithmic branch point. It should be noticed that it is sufficient to specify that particular sheet (there exists only a single one) on which $I(u,s)$ is regular at u_+ or u_- (or both), since the function will be singular on all the others. We conclude the discussion of the singularity structure of $I(u,s)$ for $s < 0$ by computing the discontinuity across the branch point at $u = 0$; to this effect we continue $I(u,s)$ in the form (II.26a) or (II.26c) to the points $u = u_0 \pm i\epsilon$, where $u_0 < 0$ (they are located on the leading sheet); the phase of z then becomes $\exp(\mp i\pi)$, so that

$$I(u_0 \pm i\epsilon, s) = \frac{i}{\sqrt{K(u_0, s, m^2)}} \ln\left(\frac{u_0+s-m^2-\sqrt{K(u_0,s,m^2)}}{u_0+s-m^2+\sqrt{K(u_0,s,m^2)}}\right)\exp(i\pi)\exp(\mp i\pi). \tag{II.28}$$

(By convention we shall always exhibit the phase of z explicitly; thus any positive quantity appearing in the argument of the log will be taken to have zero phase.) The discontinuity is therefore given by

$$[\Delta_u I(u,s)]_{u=0} = 2\pi/[K(u,s,m^2)]^{\frac{1}{2}} \quad . \tag{II.29}$$

Upon substituting this result into (II.12b) we retrieve formula (II.20a).

b. $s > 0$

We now wish to examine $I(u,s)$ for $s > 0$; from the above discussion we expect the following to happen: as we increase s through negative values, the complex singularities of $I(u,s)$ located at $u = (m \pm i\sqrt{-s})^2 \equiv u_\pm$ will move towards the real axis, which they reach for $s = 0$; their motion will proceed, however, on different sheets of the logarithmic branch point at $u = 0$. For $s > 0$, the singularities will appear on the real u axis at $u = (m + \sqrt{s})^2 \equiv u_+$ and $u = (m - \sqrt{s})^2 \equiv u_-$ [notice that u_+ and u_- as defined here are not necessarily the respective continuations of the above complex locations of the singularities; this depends upon the continuation chosen for the function $\sqrt{-s}$. Thus if we continue $I(u,s)$ from negative s to positive s using a $- i\epsilon$ prescription, then the singularity at $u = (m + \sqrt{s})^2$ will appear on the leading sheet, while that at $u = (m - \sqrt{s})^2$ will appear on all the remaining sheets of the logarithmic branch point; the opposite conclusions hold if we had used a $+ i\epsilon$ prescription; it is, however, not hard to see that either continuation will lead in the end to the same conclusions, since

our choice of displacing the contour C_z of the integral (II.10) slightly into the upper half of the k_z plane was arbitrary, and we could have just as well displaced it into the lower half of the complex plane; in fact, the motion of the singularities in the k_z plane is entirely symmetric with regard to either one of the continuations for $\sqrt{-s}$] . All the continuations of $I(u,s)$ in u will be made starting from the point $u = u_0 + i\epsilon$, lying just above the negative real axis on the leading logarithmic sheet. As we continue (II.28) to $s > 0$, the argument of the log acquires the phase $\exp(\mp i\pi)$ due to the vanishing of the denominator at $s = 0$; the upper sign corresponds to the continuation: $\sqrt{-s} = i\sqrt{s}$ and the lower to $\sqrt{-s} = -i\sqrt{s}$; we hence arrive at the following expression for $I(u,s)$ for $s > 0$:

$$I(u_0 + i\epsilon, s) = \frac{1}{\sqrt{K(u_0,s,m^2)}} \ln\left(\frac{\sqrt{K(u_0,s,m^2)} - (u_0 + s - m^2)}{\sqrt{K(u_0,s,m^2)} + (u_0 + s - m^2)}\right) \exp(\mp i\pi) , \qquad s > 0,\ u_0 < 0 . \tag{II.30}$$

We now examine the singularity structure of $I(u,s)$ at $u = u_\pm$ for two different domains of s:

c. $0 < s < m^2$

As we continue $I(u,s)$ in u along the path P shown in Fig. 27a, the phase of z [where z is defined by (II.27)] at $u = u_1$ becomes $\exp(+i\pi)$ due to the vanishing of the denominator of the argument of the log at $u = 0$ (in Figs. 27a,b the points $u = u_1$

are denoted by the subscript "i", where $i = 1,2,3,4$); hence at that point $z = |z_1| \exp(+ i\pi)$; similarily one may easily verify that, at $u = u_2$, $z = (1/|z_1|) \exp(+ i\pi)$; the discontinuity of $I(u,s)$ across $u = (m - \sqrt{s})^2$ therefore becomes

$$I(u_1,s) - I(u_2,s) = \begin{cases} 0 & \text{for } \sqrt{-s} = i\sqrt{s}\,, \\ -4\pi/[K(u_1,s,m^2)]^{\frac{1}{2}} & \text{for } \sqrt{-s} = -i\sqrt{s}\,. \end{cases}$$

We therefore find that for the continuation $\sqrt{-s} = i\sqrt{s}$, $I(u,s)$ is regular at $u = (m - \sqrt{s})^2 \equiv u_-$ if this point is located on the leading sheet, and singular at this point on all the remaining sheets of the logarithmic branch point at $u = 0$. If, on the other hand, we had chosen to continue $\sqrt{-s}$ according to a $+ i\epsilon$ prescription, then $I(u,s)$ would be found to be singular at $u = u_-$ on every sheet of the logarithmic branch point except for the one reached by a counterclockwise continuation around $u = 0$, starting from a point on the contour C_u, say [this can be easily verified by noticing that as u encircles the origin N times, the quantity z, defined in (II.27), acquires the phase $\exp(\pm 2iN\pi)$, where the upper sign corresponds to a clockwise and the lower to a counterclockwise continuation]. Next we compute the discontinuity of $I(u,s)$ across the point $u = (m + \sqrt{s})^2$ according to the path prescription P' of Fig. 27b. For $(m - \sqrt{s})^2 < u < (m + \sqrt{s})^2$, z is of the form

$$z = \left(\frac{a - ib}{a + ib}\right) \exp(+ i\pi) = \exp(i\varphi) \exp(+ i\pi)\,.$$

By following the phase of z along the path P' we find that

$$z_3 = \exp(i\varphi_3)\exp(+i\pi)$$

and

$$z_4 = \exp(-i\varphi_3 - 4i\pi)\exp(+i\pi) .$$

The discontinuity therefore becomes

$$I(u_3,s) - I(u_4,s) = \begin{cases} 4i\pi/\left|\sqrt{K(u_3,s,m^2)}\right| & \text{for } \sqrt{-s} = i\sqrt{s}, \\ 0 & \text{for } \sqrt{-s} = -i\sqrt{s} . \end{cases} \qquad \text{(II.31)}$$

which is in agreement with our expectations. Once again one may verify that for the choice $\sqrt{-s} = i\sqrt{s}$, the singularity at $u = (m + \sqrt{s})^2$ is absent from the sheet reached by a counterclockwise continuation of $I(u,s)$ around the branch point at $u = 0$.

d. $s > m^2$

The analysis of the singularity structure of $I(u,s)$ for $s > m^2$ proceeds along lines similar to those above; in contradistinction to the previous case, however, it is the numerator in the argument of the log of formula (II.30) which will vanish at $u = 0$; hence for $0 < u < (m - \sqrt{s})^2$, z has the phase $\exp(-i\pi)$; the discontinuity across $u = (m - \sqrt{s})^2$ is now computed as before; we find

$$I(u_1,s) - I(u_2,s) = \begin{cases} 4\pi/[K(u_1,s,m^2)]^{\frac{1}{2}} & \text{for} \quad \sqrt{-s} = i\sqrt{s}\ , \\ 0 & \text{for} \quad \sqrt{-s} = -i\sqrt{s}\ . \end{cases}$$

Substituting this result into (II.12b), we retrieve formula (II.20b). As an additional check we can compute the discontinuity of $I(u,s)$ between the points $u_0 + i\epsilon$ and $u_0 - i\epsilon$ $(u_0 < 0)$ according to the path prescription P of Fig. 27a for the case where $I(u,s)$ is singular at $u = (m - \sqrt{s})^2$ on the leading sheet (that is, for the continuation $\sqrt{-s} = i\sqrt{s}$). A similar analysis to that above leads once again to formula (II.29); this is in agreement with the result obtained in Section 4, according to which this discontinuity is the same for $s < m^2$ and $s > m^2$. Finally we calculate the discontinuity of $I(u,s)$ between the points $u = u_3$ and $u = u_4$ according to the path prescription P' of Fig. 27b; the analysis is quite similar to the one discussed for $s < m^2$, except that now we find that $z_3 = \exp(i\varphi_3)\exp(-i\pi)$ and $z_4 = \exp(-i\varphi_3)\exp(-i\pi)$; the discontinuity of $I(u,s)$ for the two possible continuations of $\sqrt{-s}$ around the branch point at $s = 0$ is once again given by (II.31). The singularity structure of $I(u,s)$ on the remaining sheets of the logarithmic branch point may also be readily obtained; we shall limit ourselves to merely stating the result: For the choice $\sqrt{-s} = i\sqrt{s}$, $I(u,s)$ is regular at $u = (m - \sqrt{s})^2$ and $u = (m + \sqrt{s})^2$, where these points are located on the sheet reached by a counterclockwise

continuation around the branch point at $u = 0$, and singular on all the remaining sheets of the log; if, on the other hand, we chose the continuation $\sqrt{-s} = -i\sqrt{s}$, then $I(u,s)$ would be found to be regular at the above-mentioned points if they are reached via the paths P and P' of Figs. 27a,b, and singular on all the remaining sheets of the branch point at $u = 0$. In Figs. 28a,b, and c we have summarized the situation for $s < 0$, $0 < s < m^2$, and $s > m^2$. Since, as we have pointed out before, there exists only a single sheet of the logarithmic branch point on which $I(u,s)$ is regular at $u = u_+$ or u_- or both, it is sufficient to specify that particular sheet. The paths of continuation leading to regular points of $I(u,s)$ have been indicated in the above-mentioned figures by either a solid or dashed line, depending on whether a $-i\epsilon$ or $+i\epsilon$ prescription was used for the continuation of the function $\sqrt{-s}$ around $s = 0$; all paths are shown starting at a point $u_0 + i\epsilon$, lying just above the negative u axis on the leading sheet.

6. Concluding Remarks and Summary

It was shown in Section 2 that the AFS approximation to the amplitude associated with the diagram of Fig. 1 can be written in the form

$$[A(s,t)]_{AFS} = \frac{i}{2} \int_{C_u} du\, c(u,s)\, [\exp(-i\pi\alpha(u)) \pm 1]\, t^{\alpha(u)-1}/\sin \pi\alpha(u), \tag{II.32}$$

where $c(u,s)$ is given by (II.12b) and (II.26a,c); the + or - signs are to be taken depending on whether we exchange a Regge pole of even or odd signature. For $s < m^2$ the contour C_u extends around the logarithmic branch point of $c(u,s)$ at $u = 0$ along the negative u axis; the asymptotic behaviour of (II.32) was then shown to be of the form

$$[A(s,t)]_{AFS} \sim t^{\alpha(0)-1}/\ln t \; .$$

Assuming that the AFS amplitude has a Sommerfeld-Watson representation [i.e., that it can be written in the form (I.6)], we then conclude that in the j plane of the s reaction the leading singularity of $b(j,s)$ is located at $j = \alpha(0)-1$ for $s < m^2$, and, furthermore, that near this singularity, $b(j,s) \sim$ constant $\times \ln(j - \alpha(0) + 1)$. As we increase s beyond $s = m^2$, the singularity of $c(u,s)$ at $u = (\sqrt{s}-m)^2$, which for $s < m^2$ was located on another sheet of the logarithmic branch point at $u = 0$, moves up onto the leading sheet via the branching at $u = 0$, pulling the contour to the right as we keep

increasing s. Thus for $s > m^2$, the new asymptotic behaviour of (II.32) is determined by the singularity at $u = (\sqrt{s}-m)^2$; we found it to be of the form

$$[A(s,t)]_{AFS} \sim t^{\alpha((\sqrt{s}-m)^2)-1}/(\ln t)^{\frac{1}{2}} .$$

From here we conclude that for $s > m^2$ a new singularity located at $j = \alpha((\sqrt{s} - m)^2) - 1$ must have appeared on the physical j sheet of the s reaction via the logarithmic branch point at $j = \alpha(0) - 1$, and, furthermore, that near that singularity, $b(j,s) \approx \text{const.} \times \times [j - \alpha((\sqrt{s} - m)^2) + 1]^{-\frac{1}{2}}$. The location of the singularities as well as their logarithmic and square-root nature agrees with the results obtained by Mandelstam,[2] Wilkin,[4] Gribov et al.,[5] and Simonov,[7] in connection with the single Regge pole exchange diagram for which the cancellation of the cuts does not occur (see Fig. 2, for example).

Before closing this section we wish to make two further remarks concerning (a) the signature of the partial-wave amplitude in which the leading branch points appear, and (b) the generation of the normal threshold branch points in s of the amplitude $[A(s,t)]_{AFS}$. We begin with a discussion of the first-mentioned point. Let us rewrite (II.32) as

$$[A(s,t)]_{AFS} = \frac{i}{2t} \int_{C_u} du\, c(u,s)\, [(-t)^{\alpha(u)} \pm t^{\alpha(u)}]/\sin \pi\alpha(u) .$$

We see from this expression that for large t, $[A(s,t)]_{AFS}$ is even or odd under the transformation $t \to -t$ depending on whether we exchange a Regge pole of odd or even signature, respectively; since the amplitude can always be written in the form (I.2), we conclude that in the limit of large t only the positive (negative) signature amplitude will contribute to $[A(s,t)]_{AFS}$ if we exchange a Regge pole of negative (positive) signature. Thus the leading branch point in the angular momentum plane appears in the analytically continued partial-wave amplitude of signature opposite to that of the exchanged Regge pole.

We now turn to the second point and show how the normal threshold branch points of $[A(s,t)]_{AFS}$ in s are generated; they are expected to result from the coincidence of the poles and normal threshold branch points of the Regge pole amplitude with the pole of the propagator associated with the elementary particle exchange; as we have seen, the latter manifests itself in the singularity of $c(u,s)$ at $u = (\sqrt{s} - m)^2$. We notice first of all that the integrand of (II.32) will have poles at $u = M_i^2$, where M_i are the masses of <u>physical</u> bound states or resonances lying on the Regge trajectory; they are a solution to

$$\alpha^+(M_i^2) = 0, 2, 4, \cdots,$$

$$\alpha^-(M_j^2) = 1, 3, 5, \cdots .$$

The residues of the poles at the remaining integers of $\alpha(u)$ vanish due to the presence of the signature factor in (II.32). Now for $s < m^2$, the contour C_u extends along the negative u axis and encircles the branch point of $c(u,s)$ at $u = 0$; as we increase s above m^2, a new singularity at $u = (\sqrt{s}-m)^2$ appears, and the contour C_u will be pinched between this singularity and the above-mentioned poles when

$$s_i = (m + M_i)^2 . \qquad \text{(II.33)}$$

Hence (II.33) gives the position of the singularities in s of $[A(s,t)]_{AFS}$ which arise from bound states and resonances lying on the Regge trajectory; they are, in fact, the two-body normal threshold branch points. The higher normal threshold branch points are generated in exactly the same way by the pinching of the contour C_u between the moving singularity at $u = (\sqrt{s}-m)^2$, and the normal threshold singularities at $u = u_N$ associated with the Regge pole; their location is given by

$$s_N = (m + \sqrt{u_N})^2 .$$

In addition to these singularities the analytically continued partial-wave amplitude, $b^{\pm}(j,s)$ will have singularities in s arising from the moving branch point at $j = \alpha((\sqrt{s}-m)^2) - 1$, as was originally pointed out by Mandelstam.[2] Their location is given by

$$s(j) = \{m + [\lambda(j+1)]^{\frac{1}{2}}\}^2 , \qquad \text{(II.34)}$$

where λ is the inverse function corresponding to α. For simplicity let us consider the case in which we exchange a trajectory of even singnature (the Pomeranchuk, for example). The singularity at $j = \alpha((\sqrt{s}-m)^2) - 1$ will then appear in the odd-signature partial-wave amplitude; thus from (II.34) we see that if j is an odd integer [$b^-(j,s)$ then coincides with the physical partial wave amplitude], then the singularity at $s(j)$ coincides with the normal threshold singularity at $s_{j+1} = (m + M_{j+1})^2$, where M_{j+1} is the mass of the bound state or resonance of spin $\sigma = j + 1$ lying on the Regge trajectory $\alpha(u)$. If, on the other hand, j is an even integer [for which the amplitude $b^-(j,s)$ is unphysical], then the singularity $s(j)$ coincides with an "unphysical" threshold corresponding to a two-body intermediate state formed by the elementary particle of mass m and an "unphysical" particle of spin $\sigma = j + 1$ (i.e., odd spin) lying on the even-signature Regge trajectory. We have seen, however, that due to the presence of the signature factor in (II.32), $[A(s,t)]_{AFS}$ has singularities in s corresponding only to physical thresholds; thus the latter singularities of $b^-(j,s)$ do not contribute to the full AFS amplitude; this is what one would have expected in the first place.

The above-described mechanism for the generation of the normal threshold branch points was quite straightforward, since we were able

to cast the amplitude into the form (II.32). The amplitude for the double Regge pole exchange diagram, on the other hand, does not suggest immediately that it can be written in this form, and we have to base our analysis on the integral representation (III.4a). In order to exhibit the similarity of the two mechanisms which generate the normal threshold branch points in the single and double Regge pole exchange diagrams, we briefly repeat the above analysis starting from the integral representation (II.10). For fixed x, and $s > m^2 - x$ the singularity structure of the integrand in the k_z plane is shown in Fig. 10b (we consider the continuation $\sqrt{-s} = i\sqrt{s}$; the case $\sqrt{-s} = -i\sqrt{s}$ leads to the same result). For simplicity we assume that $\alpha(u)$ has only a single bound state of mass M (besides the normal threshold singularities). In the k_z plane it gives rise to poles located at $k_z = \pm i\sqrt{M^2 - x}$. As we increase s above $m^2 - x$ the k_z integration contour will get pinched when the above singularity coincides with the singularity at $k_z = i(\sqrt{s} - \sqrt{m^2 - x})$ arising from the elementary exchange; the integral over k_z will thus be singular on the surface,

$$\sqrt{s} - \sqrt{m^2 - x} - \sqrt{M^2 - x} = 0 .$$

Subsequent integration over x will then generate an end-point singularity of $[A(s,t)]_{AFS}$ located at

$$s = (m + M)^2 ,$$

which is the normal threshold branch point corresponding to a two-body intermediate state formed by an elementary particle of mass m and a bound state of mass M. The nature of the singularity may be immediately obtained from the fact that the contour C_u is pinched by an inverse square-root singularity of $c(u,s)$ and a pole of $1/\sin \pi\alpha(u)$; if we split up the contour C_u into C' and C'' as shown in Fig. 29, then it is clear that the singular part of the integral arises from the contour integration around the pole so that the singularity of $[A(s,t)]_{AFS}$ is also of the inverse-square-root type. The remaining normal threshold singularities are generated in a completely analogous way; in the case of resonances lying on the Regge trajectory, the above-described mechanism will generate the corresponding two-body complex normal thresholds; since in the k_z plane the resonance poles are reached by going through the cuts located on the imaginary axis (they correspond to the normal threshold cuts of the Regge pole amplitude), it is clear that the above complex threshold singularities will appear on an unphysical sheet.

7. Cancellation of the Cuts.

In this section we wish to show that the remaining contribution to (II.6) coming from the so-far neglected singularities of $R(\alpha(k_3^2), t; k_2^2, k_4^2)$ in k_2^2 and k_4^2 will exactly cancel the branch points in the angular momentum plane found for the AFS approximation to the diagram of Fig. 1.

Consider the expression (II.6), where the k_1^2 integration has been performed:

$$A(s,t) \approx \frac{C}{4t} \int_{-\infty}^{0} dk_3^2 \frac{\pi}{\sqrt{(k_3^2+s-m^2)^2-4sk_3^2}} \int_{-\infty}^{+\infty} \frac{dk_4^2}{k_4^2-m^2+i\epsilon} \int_{-\infty}^{+\infty} dk_2^2 \frac{R(\alpha(k_3^2),t;k_2^2,k_4^2)}{k_2^2-m^2+i\epsilon} . \tag{II.35}$$

Let us begin with the k_2^2 integration; it can be shown quite generally that the singularities in the external "masses" of any Feynman amplitude must lie in the lower half of the complex plane if the remaining variables are real.[19] In particular this will apply to the singularities of R in k_2^2 and k_4^2. Thus the situation in the k_2^2 plane might look as in Fig. 30a, with the integration contour C_2 extending along the real axis. The singularity of R in k_2^2 lies in the lower half plane at $k_2^2 = a - i\mu$, say. One may easily convince oneself that the argument given below applies irrespective of the type or number of such singularities. The contour C_2 in Fig. 30a may be split up as shown in Fig. 30b. Since the integrand of (II.35) falls off like $1/(k_2^2)^2$ for large k_2^2, as was already pointed out, we may close the various integration contours at infinity. The contribution to the amplitude coming from the contour C_{AFS} (see Fig. 30b) is seen to correspond to the AFS type of approximation; at the same time we also recognize that the remaining integral along C'_{AFS} becomes the dispersion integral for the Regge pole amplitude evaluated at $k_2^2 = m^2$. The contributions from the contours C_{AFS} and C'_{AFS} are thus found to be identical in magnitude and opposite in sign; the integral therefore vanishes, as was

already evident at the start. If one continues to treat the above two contributions separately and performs the remaining integrations, one finds that a similar cancellation takes place within each of the separate pieces; the AFS approximation (II.7) is obtained by consistently ignoring the C'_{AFS} integrations.

III. THE DOUBLE REGGE POLE EXCHANGE DIAGRAM

1. The AFS Approximation, and Location of the Singularities in the j Plane

In this section we analyze the diagram of Fig. 3; for simplicity we consider the exchange of two identical Regge poles; the modifications that are required if this condition is relaxed are rather obvious and we state them at the end of the section. Since the general techniques to be used are those discussed previously, we recapitulate only the main steps and point out the features that distinguish the present case from the single Regge pole exchange case treated in Section II.

Making the same approximations to the Jacobian (II.4,5) as before, we arrive at the following expression for the leading contribution at large t to the amplitude associated with the diagram of Fig. 3:

$$A(s,t) \approx C \frac{1}{4t} \int dk_1^2\, dk_2^2\, dk_3^2\, dk_4^2\, \tau(k_1^2, k_3^2, s) \frac{1}{[k_2^2 - m^2 + i\epsilon]\,[k_4^2 - m^2 + i\epsilon]}$$

$$\times R\big(\alpha(k_1^2),\ t; k_2^2, k_4^2\big) R\big(\alpha(k_3^2),\ t; k_2^2, k_4^2\big)$$

$$\text{for} \quad s < 0\,, \tag{III.1}$$

where $\tau(k_1^2, k_3^2, s)$ is the triangle function defined in (I.9), and where the functions R are the amplitudes associated with the two Regge poles. The AFS type of approximation corresponds, as before, to ignoring the singularities of R in k_2^2 and k_4^2; closing the k_2^2

and k_4^2 integration contours in the lower half planes, we pick up the following contribution coming from the poles of the two propagators:[20]

$$[A(s,t)]_{AFS} = -\pi^2 C \int dk_1^2\, dk_3^2\, \tau(k_1^2,k_3^2,s)\, \frac{\gamma(k_1^2)}{\sin \pi\alpha(k_1^2)}\, \frac{\gamma(k_3^2)}{\sin \pi\alpha(k_3^2)}$$

$$\times\; C(k_1^2)\, C(k_3^2)\, t^{\alpha(k_1^2)+\alpha(k_3^2)-1}\,, \qquad \text{(III.2)}$$

where we have substituted formula (II.8) for the on-the-mass-shell Regge pole amplitudes [as before, $\gamma(k^2)$ is related to the full residue function $\beta(k^2)$ by (II.9)]; the coefficient $C(x)$ $[x \equiv k_1^2, k_3^2]$ is defined by

$$P_{\alpha(x)}(z) \xrightarrow[z \to \infty]{} C(x)\, z^{\alpha(x)}\,. \qquad \text{(III.3)}$$

Except for a trivial change, we treat formula (III.2) by the same recipe as was used in dealing with formula (II.7). Aside from providing us with a clearer picture as to how the asymptotic behaviour of the amplitude (III.2) is generated, it allows us to continue this expression to $s > 0$, and to establish the precise form of the asymptotic behaviour in t for all s [for $s < 0$, the latter may of course be calculated from the integral expression (III.2)]. Let us switch to a new set of integration variables, x and r, which are defined in terms of k_1^2 and k_3^2 by

$$x = k_3^2 - (1/4s)\,(k_1^2 - s - k_3^2)^2 ,$$

and

$$r = \left\{ (k_1^2 - s - k_3^2)/2\sqrt{-s} \right\} - \sqrt{-s}/2$$

(here r is related to the variable k_z used in Section II by $r = k_z - \sqrt{-s}/2$). In terms of x and r the integral (III.2) takes the form

$$[A(s,t)]_{AFS} = -\pi^2 C \int_{-\infty}^{0} \frac{dx}{\sqrt{-x}} \int_{-\infty}^{+\infty} dr \left\{ \frac{\gamma\left(x-(r+\sqrt{-s}/2)^2\right)}{\sin\pi\alpha\left(x-(r+\sqrt{-s}/2)^2\right)} \frac{\gamma\left(x-(r-\sqrt{-s}/2)^2\right)}{\sin\pi\alpha\left(x-(r-\sqrt{-s}/2)^2\right)} \times \mathcal{b}(x,r;s) \right\} t^{\alpha\left(x-(r+\sqrt{-s}/2)^2\right)+\alpha\left(x-(r-\sqrt{-s}/2)^2\right)-1} , \quad \text{(III.4a)}$$

where

$$\mathcal{b}(x,r;s) = C\left(x-(r+\sqrt{-s}/2)^2\right) C\left(x-(r-\sqrt{-s}/2)^2\right) . \quad \text{(III.4b)}$$

The function $C(x)$ is defined in (III.3). Consider the analytic structure of the integrand of (III.4) in the r plane; except for poles arising from the vanishing of the sine factors in the denominator, all singularities are due to the normal threshold branch points of the Regge trajectory, $\alpha(u)$, and residue, $\gamma(u)$; the location of the singularities in the r plane is thus given by

$$r_n = \pm\sqrt{-s}/2 \pm i\sqrt{u_n - x} , \quad \text{(III.5)}$$

where $\sqrt{u_n}$ stands for the energy of the bound states and resonances lying on the Regge trajectory, and for the normal threshold energies associated with $\alpha(u)$ and $\gamma(u)$. The above singularities are shown together with the integration contour in Fig. 31a. Next we define the angular momentum variable ℓ,[21]

$$\ell = \alpha\left(x-(r+\sqrt{-s}/2)^2\right) + \alpha\left(x-(r-\sqrt{-s}/2)^2\right) - 1 . \qquad \text{(III.6)}$$

Using the fact that $\alpha(u)$ is a real analytic function of u, and assuming that $d\alpha/du > 0$ for $u < 0$ (which is true under very general conditions as we have emphasized in Section II), one can readily map the contour C_r of Fig. 31a into the complex ℓ plane; the resulting contour C_ℓ is shown in Fig. 31b. The integral (III.4a) may thus be put into the form

$$[A(s,t)]_{AFS} = -\pi^2 C \int_{-\infty}^{0} \frac{dx}{\sqrt{-x}} \int_{C_\ell} \frac{d\ell}{(\partial\ell/\partial r)} \; B(\ell,s,x)\, t^{\ell} , \qquad \text{(III.7)}$$

here $B(\ell,s,x)$ stands for the quantity appearing within braces in the integrand of (III.4a), where r has been expressed in terms of ℓ and x through relation (III.6); notice that this latter transformation is necessarily singular, since (III.6) is invariant under the transformation $r \to -r$, where r is any complex number. This manifests itself in formula (III.7) as a singularity of the integrand at $\ell = 2\alpha(x + s/4)-1$ (corresponding to $r = 0$) which arises from the vanishing of $\partial\ell/\partial r$; in fact, it follows trivially from (III.6) that at $r = 0$

$$(\partial\ell/\partial r) = 0 \quad . \tag{III.8}$$

It is therefore evident that, for any given x, the contour C_ℓ shown in Fig. 31b is the minimizing contour, and the asymptotic behaviour of the integral over ℓ in (III.7) will be determined by the singularity at $\ell = 2\alpha(x + s/4) - 1$.

Next we wish to continue the integral (III.7) to positive values of s; to this effect it is best to return to the form (III.4a), since we have complete knowledge of the singularity structure of the integrand in the complex r plane. As we increase s through negative values the complex conjugate pairs of singularities move towards the imaginary axis, which they reach for $s = 0$; the situation for $s > 0$ will then be that shown in Fig. 31c (irrespective of the continuation chosen for $\sqrt{-s}$ around the branch point at $s = 0$). Thus, for a fixed value of x, the minimizing contour C_r remains undistorted as long as $s < 4(M^2 - x)$, where M is the mass of the lowest-lying bound state on the trajectory $\alpha(u)$; if no such state exists, then M is to be replaced by the first normal threshold energy $\sqrt{u_0} = 2m$ of the Regge pole amplitude. We shall assume for the present that there does exist such a bound state; it then follows that for $s = 4(M^2 - x)$ the contour C_r will get pinched by the pair of singularities located at $r = -i\sqrt{s}/2 + i\sqrt{M^2 - x}$ and $r = +i\sqrt{s}/2 - i\sqrt{M^2 - x}$ [the position of the singularities of the integrand of (III.4a) are given by (III.5)], and that for $s > 4(M^2 - x)$ it will appear as shown in Fig. 31d. The asymptotic behaviour of the

amplitude (III.7) will, of course, be determined by the upper limit of the x integration, i.e., $x = 0$ (notice that this point cannot be avoided by distorting the x-integration contour). We hence conclude that for $s < 4M^2$ the large-t behaviour of (III.7) is controlled by the singularity at $\ell = 2\alpha(x + s/4) - 1$ with x evaluated at zero, while for $s > 4M^2$ it is controlled by the singularity at $\ell = \alpha(M^2) + \alpha(s + M^2 - 2\sqrt{s}\sqrt{M^2 - x}) - 1$ (arising from the bound state singularity at $r = -i\sqrt{s}/2 + i\sqrt{M^2 - x}$), with x evaluated again at the upper limit of the x integration [that the latter singularity will dominate over the former follows from the fact that $\left(\frac{\partial^2 \ell}{\partial \eta^2}\right)_{\eta=0} > 0$ where $i\eta = r$, and ℓ is defined by (III.6)]. We therefore find that, except for logarithmic factors, $[A(s,t)]_{AFS}$ behaves for large t as

$$[A(s,t)]_{AFS} \approx \begin{cases} t^{2\alpha(s/4)-1} & \text{for} \quad s \leqslant 4M^2 , \\ t^{\ell_B + \alpha((\sqrt{s}-M)^2)-1} & \text{for} \quad s \geqslant 4M^2 , \end{cases}$$

where ℓ_B is the spin of the bound state. If $[A(s,t)]_{AFS}$ has a Sommerfeld-Watson representation--i.e., it can be written in the form (I.6)-- then we conclude from the above asymptotic behaviour that the continued partial-wave amplitude $b(j,s)$ must have a branch point at $j = 2\alpha(s/4) - 1$ for $s \leqslant 4M^2$, and an additional branch point at $j = \ell_B + \alpha((\sqrt{s} - M)^2) - 1$ for $s \geqslant 4M^2$; since the latter singularity has no effect on the asymptotic behaviour of the AFS amplitude for $s < 4M^2$, it must be located on another sheet of the branch point at $j = 2\alpha(s/4) - 1$. We shall see below that the above-mentioned singularities are respectively of the logarithmic

type and inverse-square-root type. They are evidently the analogs of the branch point at $j = \alpha(0) - 1$, and $j = \alpha((\sqrt{s} - m)^2) - 1$ associated with the single Regge pole exchange diagram.

2. Asymptotic Behaviour of the AFS Amplitude

We now wish to find the precise form of the asymptotic behaviour in t of the AFS amplitude (III.2). To this effect we return to formula (III.4); for $s < 4M^2$ the leading contribution at large t comes from the integration region $r \simeq 0$, $x \simeq 0$. Expanding the various trajectory functions, $\alpha(u)$, around $u = s/4$, and keeping only the linear terms, we obtain

$$[A(s,t)]_{AFS} \to -2\pi^2 C \left(\frac{\gamma(s/4)}{\sin\pi\alpha(s/4)}\right)^2 \mathcal{b}(0,0,s) \; t^{2\alpha(s/4)-1}$$

$$\times \int_{-x_0}^{0} \frac{dx}{\sqrt{-x}} \int_{-r_0}^{0} dr \; t^{2\alpha'[x-r^2]} + O\left(t^{2\alpha(s/4)-1-2\alpha'[r_0^2+x_0]}\right), \qquad \text{(III.9)}$$

where $\alpha' \equiv (d\alpha/du)_{u=s/4}$, x_0 and r_0 are small positive quantities, and where we have approximated the remainder of the integrand by its value at $u = s/4$. Making a change of variables one can cast (III.9) into the form

$$[A(s,t)]_{AFS} \approx B(s) \left[t^{2\alpha(s/4)-1}/\ln t\right] \; \mathrm{erf}(\sqrt{2\alpha' x_0 \ln t}) \; \mathrm{erf}(\sqrt{2\alpha' r_0^2 \ln t})$$

where

$$B(s) = -\pi^3 C \left(\frac{\gamma(s/4)}{\sin\pi\alpha(s/4)}\right)^2 \mathcal{b}(0,0;s)/2\alpha' , \qquad \text{(III.10)}$$

and where $\mathrm{erf}(x)$ is the well known error function defined in (II.23). We hence obtain for the leading contribution to the AFS amplitude at large t

$$[A(s,t)]_{AFS} \approx B(s) \quad t^{2\alpha(s/4)-1}/\ell n\, t \;, \tag{III.11}$$

where $B(s)$ is given by (III.10). Comparison of formula (III.11) with the Sommerfeld-Watson representation (I.6) shows that we are dealing with a logarithmic branch point at $j = 2\alpha(s/4) - 1$, or equivalently, that the discontinuity across the complex angular momentum cut approaches a constant near the singularity. Although we were unable to cast the integral (III.7) into a contour integral of the form (II.12a), we nevertheless can write it as an integral over the discontinuity of $\tilde{c}(\ell,s)$ where this function is defined by (II.13); we have, for $s < 0$,

$$[A(s,t)]_{AFS} = \int_{2\alpha(-\infty)-1}^{2\alpha(s/4)-1} d\ell \quad \rho(\ell,s)\, t^{\ell} \;, \tag{III.12}$$

where

$$\rho(\ell,s) = -\pi^2 C \int_{-\infty}^{0} \frac{dx}{\sqrt{-x}} \int_{-\infty}^{+\infty} dr\; \delta\left[\ell - \alpha\left(x-(r+\sqrt{-s}/2)^2\right) - \alpha\left(x-(r-\sqrt{-s}/2)^2\right)+1\right]$$

$$\times\, \mathcal{b}(x,r;s) \left\{ \frac{\gamma\left(x-(r+\sqrt{-s}/2)^2\right)}{\sin\pi\alpha\left(x-(r+\sqrt{-s}/2)^2\right)} \quad \frac{\gamma\left(x-(r-\sqrt{-s}/2)^2\right)}{\sin\pi\alpha\left(x-(r-\sqrt{-s}/2)^2\right)} \right\} .$$

Here $\mathcal{b}(x,r;s)$ is defined by (III.4b). Making the same approximations as before, one readily finds that $\rho(\ell,s) \to B(s)$ as $\ell \to 2\alpha(s/4)-1$.

Thus the discontinuity function does indeed approach a constant at the singularity.

Next we consider the asymptotic behaviour of the AFS amplitude for $s > 4M^2$; the r-integration contour in (III.4a) is then to be replaced by the contour shown in Fig. 31d; the leading contribution to the amplitude at large t comes from the bound-state poles of the integrand located at $r = i\sqrt{s}/2 - i\sqrt{M^2 - x}$ and $r = -i\sqrt{s}/2 + i\sqrt{M^2 - x}$ [we are investigating the case in which $\alpha(u)$ has a bound state of mass M and spin ℓ_B]. Now for $r \approx i\sqrt{s}/2 - i\sqrt{M^2 - x}$,

$$\sin\pi\alpha\left(x-(r-i\sqrt{s}/2)^2\right) \approx 2i\pi(-1)^{\ell_B}\,\alpha'(M^2)\,(M^2-x)^{\frac{1}{2}}\,[r-i(\sqrt{s}/2-\sqrt{M^2-x})],$$

with a similar relation holding for $\sin\pi\alpha\left(x-(r+i\sqrt{s}/2)^2\right)$ near $r = -i\sqrt{s}/2 + i\sqrt{M^2-x}$; hence we arrive at the following expression for the contribution coming from the bound state poles:

$$[A(s,t)]_{AFS} \approx D(s)\;t^{\ell_B+\alpha\left((\sqrt{s}-M)^2\right)-1}/(\ell n\, t)^{\frac{1}{2}}\;, \qquad \text{(III.13a)}$$

where (III.13b)

$$D(s) = 2\,\pi^{3/2}C\;\frac{\gamma\left((\sqrt{s}-M)^2\right)}{\sin\pi\alpha\left((\sqrt{s}-M)^2\right)}\;\frac{\gamma(M^2)\,\mathcal{P}\left(0,i(M-\sqrt{s}/2);s\right)}{(-1)^{\ell_B}\,M\,\alpha'(M^2)[(\sqrt{s}/M)\,\alpha'\left((\sqrt{s}-M)^2\right)]^{\frac{1}{2}}}$$

Formula (III.13) shows that we are dealing with a branch point at $j = \ell_B + \alpha\left((\sqrt{s}-M)^2\right)-1$ of the inverse-square-root type.

One can readily generalize our discussion to the case in which we exchange two different trajectories α_1 and α_2. The analog of the singularity at $j = 2\alpha(s/4)-1$ is still determined by (III.8); the position of the singularity for $s < 0$, as shown in the appendix, is given by

$$j = \alpha_1(u) + \alpha_2\left(-(\sqrt{-s} - \sqrt{-u})^2\right)-1 , \qquad \text{(III.14a)}$$

where u is a solution to

$$\alpha_1'(u) - \alpha_2'\left(-(\sqrt{-s} - \sqrt{-u})^2\right) \frac{\sqrt{-s} - \sqrt{-u}}{\sqrt{-u}} = 0 , \qquad \text{(III.14b)}$$

while for $s > 0$, (III.14a,b) are to be replaced by

$$j = \alpha_1(u) + \alpha_2\left((\sqrt{s} - \sqrt{u})^2\right) - 1 \qquad \text{(III.14c)}$$

and

$$\alpha_1'(u) - \alpha_2'\left((\sqrt{s} - \sqrt{u})^2\right) \frac{\sqrt{s} - \sqrt{u}}{\sqrt{u}} = 0 . \qquad \text{(III.14d)}$$

For the case in which $\alpha_1 = \alpha_2$, a solution to (III.14b) is given by $u = s/4$. Let us suppose, for simplicity, that only one of the trajectory functions, say α_1, passes through a physical bound state of mass m_1 and spin ℓ_1. In the r plane of the integrand of (III.4) this gives rise to a pair of singularities which for $s > 0$, and fixed negative x, appear on the imaginary axis at the positions

$r = -i\sqrt{s}/2 \pm i\sqrt{m_1^2 - x}$. We are forced to distort the minimizing contour associated with the vanishing of $\partial\ell/\partial r$ when the singularity at $r = -i\sqrt{s}/2 + i\sqrt{m_1^2 - x}$ reaches $r = r_0$, where r_0 is a solution to (III.8); in the ℓ plane [where $\ell = \alpha_1 + \alpha_2 - 1$] this corresponds to the coincidence of the bound-state singularity at $\ell = \ell_1 + \alpha_2(s + m_1^2 - 2\sqrt{s}\sqrt{m_1^2 - x})$ and the singularity associated with the vanishing of $\partial\ell/\partial r$. Let $s = h(x)$ be the value of s at which the above collision occurs; then for $s > h(x)$ the asymptotic behaviour of the integral over ℓ in (III.7) will be controlled by the bound-state singularity. It is shown in the Appendix that the corresponding value of s at which the asymptotic behaviour of the full amplitude (III.7) changes is given as a solution to

$$\alpha_1'(m_1^2) - \alpha_2'\left((\sqrt{s}-m_1)^2\right) \frac{\sqrt{s} - m_1}{m_1} = 0 , \qquad \text{(III.14e)}$$

and that for s greater than the critical value the amplitude will be dominated at large t by the singularity at $j = \ell_1 + \alpha_2\left((\sqrt{s}-m_1)^2\right)-1$. The general picture in the angular momentum plane which is suggested by the above analysis is summarized in the following section. Finally we wish to remark that none of the above singularities will be present in the full amplitude (III.1); the mechanism responsible for their cancellation is, of course, of the same type as the one discussed in Section II in connection with the single Regge pole exchange diagram.

3. Concluding Remarks and Summary

We shall begin by summarizing the situation for the case where the two exchanged trajectories are identical. Assuming that the AFS approximation to the diagram of Fig. 3 has a Sommerfeld-Watson representation (in which case the asymptotic behaviour of the amplitude is determined by the leading singularities in the j plane), we are led to the following picture regarding the singularity structure in the j plane of the analytically continued partial-wave amplitude of definite signature: if there exists a bound state of mass M on the trajectory $\alpha(u)$, then for $s < 4M^2$ (that is, below the threshold corresponding to the two-particle intermediate state formed by the bound states of the Regge amplitudes) the leading singularity in the j plane is located at

$$j = 2\alpha(s/4) - 1 . \tag{III.15}$$

All other singularities which lie to the right of (III.15) hence must be located on an unphysical sheet. As we increase s above $4M^2$, a new singularity emerges onto the physical j sheet via the branch point at $j = 2\alpha(s/4) - 1$ and controls the asymptotic behaviour of the amplitude; its position is given by the formula

$$j = \alpha\left((\sqrt{s} - M)^2\right) + \ell_B - 1 , \tag{III.16}$$

where ℓ_B is the spin of the bound state; this is the analog of the

moving singularity $j = \alpha((\sqrt{s} - m)^2) - 1$ we found in the single Regge pole exchange case. If, on the other hand, $\alpha(u)$ has no bound state, then (III.15) remains the leading singularity for $s < 16m^2$, that is, below the four-particle production threshold (where the two pairs of particle states are associated with the elastic intermediate states of the two Regge pole amplitudes). For $s > 16m^2$ a new singularity has appeared on the physical sheet of the j plane via the branch point at $j = 2\alpha(s/4) - 1$; its location is given by the formula

$$j = \alpha(4m^2) + \alpha((\sqrt{s} - 2m)^2) - 1 . \qquad \text{(III.17)}$$

From the singularity structure of the integrand of (III.4a) in the r plane we see that no essential difference exists between the various bound-state and threshold singularities; thus we expect that any conclusions that one reaches regarding the branch points in the j plane that arise from the latter singularities must hold in the presence, or absence, of the bound-state singularities. The general picture that seems to emerge is then the following: for $s < 4M^2$ the leading singularity is given by (III.15) with new singularities of type (III.16) and (III.17) appearing on the physical j sheet via the branch point at $j = 2\alpha(s/4) - 1$ whenever s has the appropriate value for the coincidence of the singularities of type (III.16) and (III.17) with the singularity (III.15). In the present example, where we exchange two identical trajectories, the critical value of s is given by

$s = 4M^2$ and $s = 16m^2$, respectively; the appearance of a singularity of type (III.16) or (III.17) thus coincides with the corresponding opening of a new channel in the s reaction. Thus besides the branch point at $j = 2\alpha(s/4) - 1$, we expect a multitude of other singularities to be present in the angular momentum plane, which, as we keep increasing s, will each in turn appear on the physical j sheet. The picture just described agrees with the findings of Gribov et al.[5] and Simonov[7] in connection with the analog of Fig. 3 for which the cancellation of the cuts does not take place (see Fig. 4, for example). From the asymptotic expressions for the AFS amplitude, given by (III.11) and (III.13), we conclude that for $j \approx 2\alpha(s/4) - 1$, $b(j,s) \approx \ln(j - 2\alpha(s/4) + 1)$, while for $j \approx \alpha\left((\sqrt{s} - M)^2\right) + \ell_B - 1$, $b(j,s) \approx \{j - \alpha\left((\sqrt{s} - M)^2\right) - \ell_B + 1\}^{-\frac{1}{2}}$.

The general situation where we exchange two different trajectories α_1 and α_2 is very similar to the one just described, except for a few modifications; thus the analog of (III.15) is the singularity at

$$j = \alpha_1(u) + \alpha_2\left((\sqrt{s} - \sqrt{u})^2\right) - 1 , \qquad \text{(III.18a)}$$

where u is a solution to

$$\alpha_1'(u) - \alpha_2'\left((\sqrt{s} - \sqrt{u})^2\right) \frac{\sqrt{s} - \sqrt{u}}{\sqrt{u}} = 0 . \qquad \text{(III.18b)}$$

If we assume that there exists a bound state of mass m_1 and spin ℓ_1 which lies on the trajectory α_1, then this will give rise to a singularity in the j plane located at

$$j = \ell_1 + \alpha_2\left((\sqrt{s} - m_1)^2\right) - 1 . \qquad \text{(III.19)}$$

The value of s for which this singularity will emerge onto the physical j sheet via the branch point (III.18) is now given as a solution to

$$\alpha_1'(m_1^2) + \alpha_2'\left((\sqrt{s} - m_1)^2\right) \frac{m_1 - \sqrt{s}}{m_1} = 0 . \qquad \text{(III.20)}$$

This corresponds to the coincidence of the two singularities (III.19) and (III.18). In a similar manner the lowest threshold branch point associated with the exchange of the Regge trajectory $\alpha_1(u)$ will give rise to a singularity of type (III.19) with $\ell_1 \to \alpha_1(4m^2)$ and $m_1 \to 2m$; this singularity appears on the physical sheet of the angular momentum plane at a value of s given by (III.20) with the replacement $m_1 \to 2m$. Except for modifications of the above-mentioned type, the picture in the angular momentum plane is the same as that obtained in the case for $\alpha_1 = \alpha_2$.

So far we have not specified which of the two signature amplitudes, $b^{\pm}(j,s)$, carries the above-mentioned branch points. To find an answer to this question we notice that

$$\xi_{\pm}(\alpha_1)\, \xi_{\pm}(\alpha_2)\, t^{\alpha_1+\alpha_2-1} = \frac{1}{t}\left[(-t)^{\alpha_1} \pm t^{\alpha_1}\right]\left[(-t)^{\alpha_2} \pm t^{\alpha_2}\right] .$$

It follows that the amplitude (III.4a) is even or odd under the transformation $t \to -t$ depending on whether we exchange two Regge poles of

opposite or equal signatures, respectively [we had omitted the signature factors in (III.4a)]. The amplitude (III.4a) therefore contributes for large t to only one of the terms in the sum (I.2); we hence conclude that the above-mentioned branch points in the angular momentum plane will appear in the even or odd signature partial-wave amplitudes associated with the s reaction depending on whether the two exchanged trajectories have opposite or equal signatures (in that order).

Concerning the normal threshold singularities in s of $[A(s,t)]_{AFS}$, they are generated in a way entirely analogous to the single Regge pole exchange case. Thus, let us suppose that there exist two physical bound states of masses m_1 and m_2 which lie on the trajectories α_1 and α_2, respectively. For $s > 0$ the pairs of singularities of the integrand of (III.4a) in the r plane arising from each of the bound states will lie along the imaginary axis; as we keep increasing s, two of the four singularities (one from each pair) will pinch the r-integration contour when

$$\sqrt{s} - \sqrt{m_1^2 - x} - \sqrt{m_2^2 - x} = 0 .$$

Performing the x integration then generates an end-point singularity of $[A(s,t)]_{AFS}$ at

$$s = (m_1 + m_2)^2 .$$

This is the normal threshold branch point corresponding to the two-body intermediate state formed by the bound states of mass m_1 and m_2. As we increase s above $s = (m_1 + m_2)^2$, the r-integration contour will again be pinched between the bound-state singularities and one from each pair of threshold singularities that arise from the normal threshold branch points of the Regge pole amplitudes, when either

$$\sqrt{s} - \sqrt{m_1^2 - x} - \sqrt{4m^2 - x} = 0$$

or

$$\sqrt{s} - \sqrt{m_2^2 - x} - \sqrt{4m^2 - x} = 0 .$$

Subsequent integration over x then produces the corresponding three-body normal threshold singularities at $s = (m_1 + 2m)^2$, and $s = (m_2 + 2m)^2$, respectively. The generalization of this result is self-evident [if there are resonances lying on the trajectories α_1 and α_2, they will give rise to complex normal thresholds on the unphysical s sheet; the latter follows from the fact that in the r plane the corresponding singularities are reached by going through the cuts associated with the singularities that arise from the normal threshold branch points of the trajectory functions $\alpha_1(u)$ and $\alpha_2(u)$, and residue functions $\gamma_1(u)$ and $\gamma_2(u)$].

IV. DIAGRAMS THAT HAVE THE MANDELSTAM SINGULARITIES

So far we have dealt with a set of Feynman graphs which in an AFS type of approximation gave rise to angular momentum branch points that are, however, absent in the full amplitude. Nevertheless we have studied them in great detail for two reasons: (a), we wished to obtain a clearer understanding of the mechanism responsible for the cancellation of the cuts (which presumably is not in operation for such diagrams as shown in Figs. 2 and 4); and (b), we expect that the location and nature of the singularities found for the AFS type of approximation to the diagrams of Figs. 1 and 3 is the same as that found for the full amplitudes associated with the diagrams of Figs. 2 and 4, the roles played by the "crosses" (which replace the original elementary lines) being essentially that of preventing the above-mentioned cancellation mechanism from operating. It is clear that the complexity of the latter diagrams will make it impossible to carry out as careful an analysis as was made for their simpler versions, and we will have to sacrifice a certain amount of rigour in favor of simplicity. We shall be mainly concerned with the diagram of Fig. 2, which was shown by Mandelstam[2] to have the singularity at $j = \alpha\left((\sqrt{s} - m)^2\right) - 1$ found for the AFS type of approximation to the diagram of Fig. 1 (see Section II). The double Regge pole exchange case can then be treated in a completely analogous way, and we shall limit ourselves to a statement of the result.

Consider the Feynman amplitude corresponding to the diagram of Fig. 2:

$$A(s,t) = -i\left(\frac{g}{4\pi^2}\right)^6 \int d^4\xi_1\, d^4k_1\, d^4\eta_1 \; \frac{1}{\eta_1^2 - m^2 + i\epsilon} \prod_{i=1}^{4} \frac{1}{[\xi_i^2 - m^2 + i\epsilon][k_i^2 - m^2 + i\epsilon]}$$

$$\times\; R\left(\alpha(\eta_2^2),\, U;\, \xi_3^2,\, \xi_4^2,\, k_3^2,\, k_4^2\right), \qquad \text{(IV.1)}$$

where $R\left(\alpha(\eta_2^2),\, U;\, \xi_3^2,\, \xi_4^2,\, k_3^2,\, k_4^2\right)$ is the amplitude associated with the Regge pole, U being the momentum transfer variable defined by

$$U = (\xi_3 + k_3)^2 = (\xi_4 + k_4)^2 . \qquad \text{(IV.2)}$$

Let

$$s' = \eta_2^2 ,$$

$$s'' = \eta_1^2 ,$$

$$t' = (q_1 + \eta_2)^2 ,$$

$$t'' = (q_2 - \eta_2)^2 .$$

The components of the four-vector η_1 may be expressed in terms of the invariants s', s'', t', and t''; the Jacobian for the transformation is given as before by (II.4) and (II.5) with the replacements $k_1^2 \to s''$, $k_3^2 \to s'$, $k_2^2 \to t'$, $k_4^2 \to t''$; proceeding as in Section II, we will keep only the first two terms in the expression for D [see Eq. (II.5)]

for $t \to \infty$ and small momentum transfers s ; with this approximation our integral (IV.1) becomes

$$A(s,t) \xrightarrow[t\to\infty]{} -\frac{i}{4}\left(\frac{g}{4\pi^2}\right)^6 \frac{1}{t}\iint ds'\, ds'' \;\frac{\tau(s,s',s'')}{s''-m^2+i\epsilon}$$
$$\times\left[\int_{-\infty}^{+\infty} dt' \int_{-\infty}^{+\infty} dt''\; F(s',s'',t',t'';s,t)\right], \tag{IV.3}$$

where $\tau(s,s',s'')$ is the usual triangle function defined in (I.9), and where

$$F(s',s'',t',t'';s,t) = \int d^4\xi_1\, d^4k_1 \prod_{i=1}^{4} \frac{R\left(\alpha(s'),U;\xi_3^2,\xi_4^2,k_3^2,k_4^2\right)}{[\xi_i^2-m^2+i\epsilon][k_i^2-m^2+i\epsilon]}\,. \tag{IV.4}$$

Now among the many singularities of $F(s',s'',t',t'';s,t)$ there are those pertaining to the integral (IV.1) with R replaced by a constant; i.e., it has the singularities of

$$\tilde{F}(s',s'',t',t'';s) = A^C(s,t';s',s'')\, A^C(s,t'';s',s'')\,,$$

where $A^C(s,t';s',s'')$ is the invariant amplitude associated with the "cross" in Fig. 2 when the Regge pole is replaced by an elementary line of "mass" s':

$$A^C(s,t';s',s'') = \int d^4\xi_1 \prod_{i=1}^{4} \frac{1}{\xi_i^2-m^2+i\epsilon}\,. \tag{IV.5}$$

Now $A^C(s,t';s',s'')$ has normal threshold branch points at

$$t' = 4m^2 - i\epsilon$$

and

$$u' \equiv (\eta_2 - p_1)^2 = 4m^2 - i\epsilon ,$$

with similar relations for the normal threshold branch points of $A^C(s,t'';s',s'')$ in t'' and u'', where we have the following constraint among t', u' and t'', u'':

$$t' + u' + s = t'' + u'' + s = 2m^2 + s' + s''.$$

It follows that $F(s',s'',t',t'';s,t)$ will be singular at

$$t' = 4m^2 - i\epsilon \tag{IV.6a}$$

and

$$t' = s' + s'' - s - 2m^2 + i\epsilon , \tag{IV.6b}$$

with an identical set of singularities of F in the variable t''. The singularities (IV.6a,b) correspond to those of the contracted Feynman diagrams shown in Figs. 32a,b. The essential feature to be noticed about them is that they appear on opposite sides of the t' integration contour, $C_{t'}$, just below and above the real axis (the same, of course, applies to the singularities of F in t''); the integration contours in the t' and t'' planes are thus forced to cross the real axis somewhere between t' (or t'') $= 4m^2$ and

t' (or t'') $= s' + s'' - s - 2m^2$. Now the singularities of F at $t' = 4m^2 - i\epsilon$ and $t'' = 4m^2 - i\epsilon$ arise from a pinch of the integration contours in (IV.4); furthermore, it follows from the Landau conditions for these singularities that at the pinch

$$\left.\begin{aligned} \xi_2 &= -\xi_4 \\ \xi_2^2 &= \xi_4^2 = m^2 \end{aligned}\right\} \quad ; \quad t' = 4m^2 - i\epsilon \qquad \text{(IV.7a)}$$

and

$$\left.\begin{aligned} k_2 &= -k_4 \\ k_2^2 &= k_4^2 = m^2 \end{aligned}\right\} \quad ; \quad t'' = 4m^2 - i\epsilon \ . \qquad \text{(IV.7b)}$$

Hence, from (IV.7a,b) we see that at $t' = t'' = 4m^2 - i\epsilon$ there exists a region of integration in (IV.4), which cannot be avoided, where ξ_2, ξ_4, k_2, and k_4 are on their mass shells and the integrand "blows up." In addition one may verify from (IV.7a) and (IV.7b) that, at the multiple pinch corresponding to $t' = t'' = 4m^2 - i\epsilon$, $U = t/4$, where U is defined by (IV.2). Analogous relations to (IV.7a,b) exist for the singularities at $t' = t'' = s' + s'' - s - 2m^2 + i\epsilon$:

$$\left.\begin{aligned} \xi_1 &= -\xi_3 \\ \xi_1^2 &= \xi_3^2 = m^2 \end{aligned}\right\} \quad ; \quad t' = s' + s'' - s - 2m^2 + i\epsilon \qquad \text{(IV.7c)}$$

and

$$k_1 = -k_3 \qquad ; \quad t'' = s' + s'' - s - 2m^2 + i\epsilon \quad . \qquad \text{(IV.7d)}$$
$$k_1^2 = k_3^2 = m^2$$

Once again we find that, at the multiple pinch corresponding to $t' = t'' = s' + s'' - s - 2m^2 + i\epsilon$, $U = t/4$. Now, as we have already noted, the integration contours in the t' and t'' planes are constraint to cross the real axis somewhere between t' (or t'') $= 4m^2$, and t' (or t'') $= s' + s'' - s - 2m^2$. From (IV.3) we see, however, that the s' and s'' integration includes the region where $s' \simeq 0$, and $s'' \simeq s$; since $s' = 0$, $s'' = s$ is a point on the boundary of the domain of integration

$$s^2 + s'^2 + s''^2 - 2ss' - 2ss'' - 2s's'' = 0 ,$$

we cannot distort the s' and s'' integration contours so as to avoid it. Now at $s' = 0$, $s'' = s$, the singularities of F in t' and t'' are located at $t' = t'' = 4m^2 - i\epsilon$, and $t' = t'' = -2m^2 + i\epsilon$; their separation is thus "small" and one might expect that, in this region of the "approximate pinch," $\xi_i^2 \approx k_i^2 \approx m^2$, and $U \approx t/4$. Now it does not seem totally unreasonable to assume that the major contribution to the quantity appearing within the square brackets in (IV.3) comes from the above-mentioned region of the "approximate pinch" in the t' and t'' planes, and from the integration region of (IV.4)

for which all four-momenta squared are close to their mass shell value. Thus one might try to approximate the function $R(\alpha(s'), U; \xi_3^2, \xi_4^2, k_3^2, k_4^2)$ in (IV.4) by its value for $U = t/4$, and $\xi_3^2 = \xi_4^2 = k_3^2 = k_4^2 = m^2$; with this approximation the integral (IV.3) becomes

$$A(s,t) \underset{t\to\infty}{\approx} -\frac{i}{4}\left(\frac{g}{4\pi^2}\right)^6 \frac{1}{t}\iint ds'\, ds'' \; \frac{\tau(s,s',s'')}{s''-m^2+i\epsilon}\; R(\alpha(s'), t/4) \times \left[\int_{-\infty}^{+\infty} dt'\, A^C(s,t';s',s'')\right]^2 , \tag{IV.8}$$

where $A^C(s,t';s',s'')$ is given by (IV.5). Formula (IV.8) is very similar to that corresponding to the AFS approximation to the amplitude associated with the diagram of Fig. 1 which is given by (II.7). Before proceeding with the analysis of (IV.8) we wish to emphasize once more that the existence of the "approximate pinch" in the t' <u>and</u> t'' planes was essential in the derivation of expression (IV.8); this in turn requires that both the right <u>and</u> left-hand portions of the diagrams must have a third double spectral function with respect to the s reaction; since this is not the case for the diagrams of Figs. 5, 6, and 7, the above-given arguments leading from (IV.3) to formula (IV.8) do not apply; in fact, it has been shown by Wilkin[4] that if either the right or the left-hand portion of the diagram does not have a third double spectral function, one can distort the integration contours of the Feynman amplitude (IV.1) in such a way that the Regge pole will not assume its characteristic asymptotic form anywhere along the paths of integration.

We now return to formula (IV.8) and extract from it the leading term for $t \to \infty$ which comes from the integration region where $s' \simeq 0$, and $s'' \simeq s$. Approximating $A^C(s,t';s',s'')$ by $A^C(s,t';0,s)$ in this domain, and proceeding as in Section II, we obtain, upon substituting (II.8) for R,

$$A(s,t) \approx -\frac{i}{16}\left(\frac{g}{4\pi^2}\right)^6 \frac{\gamma(0)}{\sin\pi\alpha(0)} [K(s)]^2\, C(\alpha)\xi_{\pm}(\alpha)\left(\frac{t}{4}\right)^{\alpha(0)-1} \int_{-\epsilon}^{0} ds' \left(\frac{t}{4}\right)^{\alpha'(0)s'}$$

$$\times \int ds'' \frac{\tau(s,s',s'')}{s''-m^2+i\epsilon} \qquad \text{(IV.9a)}$$

$$\approx \frac{i\pi}{16}\left(\frac{g}{4\pi^2}\right)^6 \frac{\gamma(0)}{\sin\pi\alpha(0)} \frac{[K(s)]^2}{m^2-s} C(\alpha)\xi_{\pm}(\alpha)\left(\frac{t}{4}\right)^{\alpha(0)-1} / \alpha'(0)\ln(t/4),$$

where $C(\alpha) \equiv C(\alpha(0))$ and $\xi_{\pm}(\alpha) = \xi_{\pm}(\alpha(0))$ are defined by (I.5) and (I.7), and

$$K(s) = \int_{-\infty}^{+\infty} dt'\; A^C(s,t';0,s)\,. \qquad \text{(IV.9b)}$$

1. An Estimate of the Contribution Coming From the Leading Angular Momentum Branch Point of the Double Regge Pole Exchange Diagram.

The diagram involving the exchange of two Regge poles (see Fig. 4) can be dealt with in exactly the same way as above; for simplicity we shall consider the case of two identical Regge poles. Making the same type of approximations as before, one arrives at the following expression for the amplitude:

$$A(s,t) \underset{t\to\infty}{\approx} \frac{i}{4}\left(\frac{g}{8\pi^3}\right)^4 \frac{1}{t}\iint ds'\, ds''\;\; \tau(s,s',s'')\, R\big(\alpha(s'),\, t/4\big)$$

$$\times\, R\big(\alpha(s''),\, t/4\big)\left\{\int_{-\infty}^{+\infty} dt'\; A^C(s,t';s',s'')\right\}^2 \quad ; \tag{IV.10}$$

the leading contribution to (IV.10) comes from the integration region $s' \approx s'' \approx s/4$, so that we may approximate $A^C(s,t';s',s'')$ by $A^C(s,t';s/4,s/4)$ in this domain. If we then substitute

$$R\big(\alpha(s),\, t/4\big) \;=\; \tilde{\gamma}(s)\; C(\alpha)\; \xi_{\pm}(\alpha)(t/4\bar{t})^{\alpha(s)}/\sin \pi\alpha(s) \tag{IV.11}$$

into Eq. (IV.10) [here $\bar{t}$ is a reference energy to be specified below] and make the change of variables $\xi = s'+ s''$, $\eta = s'- s''$, we arrive at the following formula for the asymptotic contribution to $A(s,t)$:

$$A(s,t) \approx \frac{i}{32}\left(\frac{g}{8\pi^3}\right)^4 \left(\frac{\tilde{\gamma}(s/4)H(s)C(\alpha)\xi_{\pm}(\alpha)}{\sin \pi\alpha}\right)^2 \frac{1}{\bar{t}}\left(\frac{t}{4\bar{t}}\right)^{2\alpha(s/4)-1-\frac{s}{2}\alpha'}$$

$$\times \int_{\frac{s}{2}-\epsilon}^{\frac{s}{2}} d\xi \left(\frac{t}{4\bar{t}}\right)^{\alpha'\xi} \int d\eta \;\; \frac{\theta(2s\xi - s^2 - \eta^2)}{\sqrt{2s\xi - s^2 - \eta^2}} \tag{IV.12a}$$

$$\approx \frac{i\pi}{32}\left(\frac{g}{8\pi^3}\right)^4 \left(\frac{\tilde{\gamma}(s/4)H(s)C(\alpha)\xi_{\pm}(\alpha)}{\sin \pi\alpha}\right)^2 \left(\frac{t}{4\bar{t}}\right)^{2\alpha(s/4)-1} / \bar{t}\alpha' \ln(t/4\bar{t}) \;,$$

where $\alpha \equiv \alpha(s/4)$, $\alpha' \equiv \alpha'(s/4)$, and

$$H(s) = \int_{-\infty}^{+\infty} dt' \; A^C(s,t';s/4,s/4) \; . \qquad \text{(IV.12b)}$$

From formulae (IV.9) and (IV.12) we see that for $s < 0$ the position of the leading branch points in the angular momentum plane for the amplitudes associated with the diagrams of Figs. 2 and 4 are given by $j = \alpha(0) - 1$ and $j = 2\alpha(s/4) - 1$, respectively; furthermore, from the form of the asymptotic behaviour we conclude that both of the above-mentioned branch points are of the logarithmic type; this is precisely the result we obtained in connection with the diagrams of Figs. 1 and 3.

Finally we wish to cast (IV.12b) into a more convenient form for computational purposes. Since we shall be interested in the value of (IV.12b) at small momentum transfers s, we will approximate the integrand by $A^C(s,t';0,0)$. Now, on account of the many approximations made in deriving formula (IV.10), we can only hope to obtain a very rough estimate of the contribution to the amplitude coming from the cut. For practical reasons we shall therefore make a further approximation and replace $A^C(s,t;0,0)$ by $A^C(s,t)$, where the latter is the amplitude associated with the "cross" with all external masses taken equal to m^2. Now, $A^C(s,t)$ is known to have the spectral representation

$$A^C(s,t) = \frac{1}{\pi^2} \int dt' \int du' \; \frac{\rho(t',u')}{(t'-t)[u'-(4m^2-s-t)]} \; , \qquad \text{(IV.13)}$$

where $\rho(t,u)$ is the well-known Mandelstam double spectral function for the box diagram;[23] the boundary of the region where $\rho(t,u) \neq 0$ is given by: $(t - 4m^2)(u - 4m^2) - 4m^4 = 0$; from here it follows that, for fixed s, (IV.13) defines an analytic function of t in the t-plane cut from $t = 4m^2$ along the positive t axis, and from $t = -s$ along the negative axis. The singularities at $t = 4m^2$ and $t = -s$ are the ones responsible for the approximate pinch discussed previously (where the limit $\epsilon \to 0$ has been taken); the contour $C_{t'}$ of the integral (IV.12b) extends just above and just below the right- and left-hand cuts, respectively; it is shown in Fig. 33a. Now for fixed s, $A^C(s,t)$ vanishes like $1/t^2$ for large t; we therefore may distort the contour C_t around the right-hand cut of $A^C(s,t)$, as shown in Fig. 33b, and rewrite the integral (IV.12b) in the form

$$H(s) \approx 2i \int_{4m^2}^{\infty} dt' \; A_t^C(s,t') \, , \qquad \text{(IV.14)}$$

where $A_t{}^C(s,t)$ is the t-channel absorptive part of $A^C(s,t)$, which, in the notation of Ref. 23, is given by

$$A_t^C(s,t) = \frac{-i\pi^3}{[K(t,u)]^{\frac{1}{2}}} \, \ell n \left(\frac{\alpha(t,u) + (q_t/\sqrt{t})[K(t,u)]^{\frac{1}{2}}}{\alpha(t,u) - (q_t/\sqrt{t})[K(t,u)]^{\frac{1}{2}}} \right) , \qquad \text{(IV.15a)}$$

where

$$K(t,u) = 4tu[tu - 4m^2(t + u) + 12m^4] ,$$

$$\alpha(t,u) = tu - 2m^2t - 4m^2u + 6m^4 ,$$

$$q_t^2 = - m^2 + t/4 , \qquad \text{(IV.15b)}$$

and

$$u = 4m^2 - s - t .$$

If, in (IV.12), α is taken to be the Pomeranchuk trajectory, then we obtain, for the contribution coming from the cut at zero momentum transfer

$$[A(0,t)]_{cut} = \frac{\pi}{128}\left(\frac{g}{8\pi^3}\right)^4 \tilde{\gamma}(0)[H(0)]^2 R(\alpha(0),t)/ \bar{t}\, \alpha'(0)\ln(t/4\bar{t}), \qquad \text{(IV.16a)}$$

where

$$R(\alpha(0),t) = - i\, \tilde{\gamma}(0)\left(\frac{t}{\bar{t}}\right) . \qquad \text{(IV.16b)}$$

Formula (IV.16) gives the contribution for large t coming from the leading angular momentum cut associated with the diagram of Fig. 4 in terms of the contribution coming from the exchange of the Pomeranchuk pole. We now wish to estimate the ratio of the two contributions. From formulae (IV.14) and (IV.15a,b) one finds, after some algebra,

$$H(0) = -\frac{\pi^3}{m^2}\int_0^\infty dz \frac{1}{(z+2)\sqrt{(z^2+4z)}} \ln[1+z(z+2)] \approx -1.53\,\pi^3/m^2 .$$

Next we shall assume that an estimate of $\tilde{\gamma}(0)$ is given by the corresponding residue function associated with the coupling of the Pomeranchuk trajectory to the $\pi - \pi$ system; the latter has been estimated in Ref. 24; taking into account that the Regge pole amplitude R used in this section is related to that of Ref. 24 (call it R') by $R = 16\pi R'$, we find that $\tilde{\gamma}(0) \approx -16\pi$, if the reference energy $\bar{t}$ in (IV.11) is chosen to be $\bar{t} = 1.87\ (\mathrm{BeV})^2$. Finally, to obtain an estimate of the coupling strength g, we take recourse to the following model: consider the amplitude for scattering of two scalar particles in the ladder approximation to the Bethe-Salpeter equation (all particles involved in the ladder are taken to have mass m); in this approximation an estimate of the coupling strength may be obtained by requiring that the leading Regge trajectory shall pass through unit angular momentum at zero energy. The calculations of Ref. 25 show that the required value of g is approximately given by $g = (16\pi)\,m$ (this corresponds to the value $\lambda = 16$ in Ref. 25). Substituting the values for $H(0)$, $\tilde{\gamma}(0)$, and g into formula (IV.16a), we find

$$A(0,t)/R(0,t) \approx -4.7/\,\bar{t}\,\alpha'(0)\,\ln(t/4\bar{t}) , \qquad \text{(IV.17)}$$

where we have written $R(0,t) \equiv R(\alpha(0),t)$. Now, there are indications that the Pomeranchuk trajectory is rather flat; if we take, for

example, its slope to be 1/3 that of the P' trajectory (which is presumed to go through angular momentum 2 at the mass of the f_0, and through 1/2 at zero energy), then we find, using formula (IV.17), that the ratio becomes unity at an energy around 140 BeV. This dominance of the cut over the pole would become even stronger as we moved away from the forward direction. Expanding the trajectory function $\alpha(s/4)$ appearing in (IV.12a) around $s = 0$, one obtains, for the ratio A/R at small momentum transfers s

$$A(s,t)/R(s,t) \approx -4.7 \exp[-\frac{s}{2} \lambda(t)]/ \bar{t} \lambda(t) , \qquad \text{(IV.18a)}$$

where

$$\lambda(t) = \alpha'(0) \ln(t/4\bar{t}). \qquad \text{(IV.18b)}$$

The above-obtained results should, of course, not be taken at their face value, in view of the numerous approximations made in the derivation of (IV.17) and (IV.18); even if, all parameters appearing in (IV.16a) were known, it would not be surprising if the true result differed from the one obtained above by an order of magnitude, or even more.

2. Conclusion

The considerations of the preceding section indicate that the location and nature of the angular momentum branch points associated with the diagrams for which the cancellation of the cuts does not occur is the same as that for the AFS approximation to their simpler versions, considered in detail in Sections II and III. The role of

the third double spectral function associated with the cross in the diagrams of Figs. 2 and 4 thus appears to be essentially that of preventing the above-mentioned cancellation from occurring; the latter diagrams have been studied in much more detail in Refs. 2 and 5 via s-channel unitarity, and the results support the above conclusions. Concerning our estimate of the contribution to the amplitude coming from the Mandelstam singularity associated with the diagram of Fig. 4, it can, of course, not be taken very seriously; it does, however, suggest that at moderate energies, the cut and pole contributions might conceivably be of the same order of magnitude. The method used in the analysis of Figs. 1 and 3 had been originally adapted to the purpose of exposing in as clear a way as possible the cancellation mechanism of the Amati, Fubini, Stanghellini cuts; this mechanism has been found to be extremely simple. The same method also led to a relatively simple analysis of the singularities in the angular momentum plane of the s reation; we found them to be of the two general types: those that are independent of particle masses, and those which depend on them. Only the former ones remain on the physical j sheet at negative momentum transfers; their positions in the j plane are given by $j = \alpha(0) - 1$ and $j = 2\alpha(s/4) - 1$ for the single and double Regge pole exchange diagrams, respectively. It is interesting to note that both these singularities are of the logarithmic type and are a consequence of the singular nature of the mapping of the k_z plane into the complex ℓ plane, where ℓ is the angular momentum in the s channel obtained by coupling the (complex) spins of the exchanged

systems to a relative orbital angular momentum $L = -1$. The analog of the singularity at $j = \alpha((\sqrt{s} - m)^2) - 1$ for the single Regge pole exchange diagram is the singularity at $j = \alpha((\sqrt{s} - M)^2) + \ell_B - 1$ associated with the diagram involving the exchange of two identical Regge poles; these singularities appear on the physical j sheet via the particle-mass independent branch points for $s > m^2$ and $s > 4M^2$, respectively; furthermore, both are of the inverse-square-root type. The similarity between the amplitudes (IV.9) and (II.7), and, (IV.10) and (III.2), suggests that the above picture in the j plane remains the same for the diagrams of Figs. 2 and 4.

In conclusion, the analysis presented in this paper indicates that everything we wish to know regarding the location and nature of the angular momentum branch points associated with the diagrams in which the singularities are not cancelled, can be learned by investigating the corresponding simpler versions of these diagrams in an AFS type of approximation; thus it appears that the additional complexity of the former diagrams, aside from modifying the strength of the singularities, merely serves to prevent the cancellation of the cuts from occurring.

ACKNOWLEDGMENTS

The author would like to express his appreciation to Professor Geoffrey F. Chew for suggesting related research topics which stimulated our interest in the present work, and for his guidance and encouragement given throughout the course of the research performed in connection with the Ph.D. degree. He also would like to thank John Schwarz and Jerome Finkelstein for several helpful discussions concerning the problems dealt with in this paper, and Cherie Beckstrom for her careful typing of the manuscript.

This work was done under the auspices of the United States Atomic Energy Commission.

APPENDIX

Position of the Branch Points in the j plane for the Case in Which Two Different Regge Trajectories are Exchanged

a. $s < 0$

For any fixed value of x the integrand of (III.7) is singular when

$$(\partial \ell / \partial r) = 0 ,$$

where ℓ is defined in terms of x and r by (III.6). In the ℓ plane the location of this singularity is given by $\ell = \lambda(x)$,

$$\lambda(x) = \alpha_1\left(x - (f + \sqrt{-s}/2)^2\right) + \alpha_2\left(x - (f - \sqrt{-s}/2)^2\right) - 1 , \qquad \text{(A.1a)}$$

where $f \equiv f(x,s)$ is a solution to

$$\alpha_1'\left(x - (f + \sqrt{-s}/2)^2\right)(f + \sqrt{-s}/2) + \alpha_2'\left(x - (f - \sqrt{-s}/2)^2\right)(f - \sqrt{-s}/2) = 0 . \qquad \text{(A.1b)}$$

We now show that, for $x < 0$,

$$\lambda(0) > \lambda(x) , \qquad \text{(A.2)}$$

so that (A.1a) takes on its maximum value at $x = 0$; since the integration contour C_ℓ of the integral (III.7) cannot be pushed to the left of $\ell = \lambda(x)$, and since the integration contour in the x plane

cannot be distorted away from $x = 0$, it is then evident from (A.2) that the asymptotic behaviour of the amplitude is determined by the value of (A.1a,b) at $x = 0$. Relation (A.2) can be verified immediately by computing the total derivative of $\lambda(x)$ with respect to x :

$$d\lambda/dx = \alpha_1'\left(x - (f + \sqrt{-s}/2)^2\right) + \alpha_2'\left(x - (f - \sqrt{-s}/2)^2\right) + (\partial\lambda/\partial f)(\partial f/\partial x);$$

now from (A.1b) we have that $\partial\lambda/\partial f = 0$; hence the last term on the right-hand side vanishes. Furthermore, the derivatives of α_1 and α_2 are positive, since it follows from (A.1b) that $-\sqrt{-s}/2 < f < \sqrt{-s}/2$, so that the arguments of the trajectory functions are negative; formula (A.2) therefore follows. From the asymptotic behaviour of the AFS amplitude (III.7) [which, as explained above, is determined by $\ell = \lambda(0)$] we then conclude that there exists a branch point in the j plane located at

$$j = \alpha_1\left(-(f + \sqrt{-s}/2)^2\right) + \alpha_2\left(-(f - \sqrt{-s}/2)^2\right) - 1 , \qquad \text{(A.3a)}$$

where f is a solution to

$$\alpha_1'\left(-(f + \sqrt{-s}/2)^2\right)(f + \sqrt{-s}/2) + \alpha_2'\left(-(f - \sqrt{-s}/2)^2\right)(f - \sqrt{-s}/2) = 0 . \qquad \text{(A.3b)}$$

Upon making the substitution $(f + \sqrt{-s}/2)^2 = -u$ in formulae (A.3a,b), we arrive at the expressions (III.14a,b) of the text.

b. $s > 0$

For concreteness sake we consider the case where $\sqrt{-s}$ is continued to $s > 0$ according to: $\sqrt{-s} = i\sqrt{s}$ (one may readily verify that the continuation $\sqrt{-s} = -i\sqrt{s}$ leads to the same results presented in the remainder of this Appendix). For $s > 0$ and fixed x, $\partial\ell/\partial r$ will then vanish for $r = ig$, where g is a solution to

$$\alpha_1'\left(x + (g + \sqrt{s}/2)^2\right)(g + \sqrt{s}/2) + \alpha_2'\left(x + (g - \sqrt{s}/2)^2\right)(g - \sqrt{s}/2) = 0 \qquad \text{(A.4a)}$$

and the location of the singularity in the ℓ plane will be given by $\ell = \tilde{\lambda}(x)$, where

$$\tilde{\lambda}(x) = \alpha_1\left(x + (g + \sqrt{s}/2)^2\right) + \alpha_2\left(x + (g - \sqrt{s}/2)^2\right) - 1 \qquad \text{(A.4b)}$$

Similar reasoning as before then leads to the conclusion that the position of the AFS singularity in the j plane is given by $j = \tilde{\lambda}(0)$, where the quantity g in (A.4b) is a solution to (A.4a) with $x = 0$. Upon making the substitution $u = (g + \sqrt{s}/2)^2$, one arrives at (III.14c,d).

c. The Critical Value of s at Which the Asymptotic Behaviour of the AFS Amplitude Changes

Let us assume, for simplicity, that only one of the trajectory functions, say α_1, passes through a physical bound state of mass m_1 and spin ℓ_1. In the r plane of the integrand of (III.4a) this gives rise to a pair of singularities which, for $s > 0$, appear on the imaginary axis at $r = ig_\pm$, where $g_\pm = -\sqrt{s}/2 \pm \sqrt{m_1^2 - x}$; these

singularities are imaged in the ℓ plane of the integrand of (III.7) into a corresponding set located at $\ell = \ell_{\mp}$, where $\ell_{\mp} = \ell_1 + \alpha_2(s + m_1^2 \mp 2\sqrt{s}\sqrt{m_1^2 - x}) - 1$; for fixed x, the value of s at which the asymptotic behaviour of the integral over ℓ in (III.7) changes then occurs when the singularity at $\ell = \hat{\lambda}(x)$ collides with the bound-state singularity at $\ell = \ell_-$, or, equivalently, when $g = g_+$ is a solution to (A.4a) [that the singularity at $\ell = \ell_+$ is not involved in the collision can be seen by noticing that $g = g_-$ (where $r = ig_-$ is the position of the singularity in the r plane corresponding to that at $\ell = \ell_+$) cannot be a solution to (A.4a)]. A moments thought then shows that the change in the asymptotic behaviour of the full AFS amplitude (III.7) [which is determined by the upper limit of the x integration] takes place when s is a solution to

$$\alpha_1'(m_1^2) - \alpha_2'\left((\sqrt{s} - m_1)^2\right) \frac{\sqrt{s} - m_1}{m_1} = 0 .$$

For s greater than the critical value, call it s_C, the large- t behaviour of the amplitude (III.7) will be determined by the above-mentioned singularity at $\ell = \ell_1 + \alpha_2\left(s + m_1^2 - 2\sqrt{s}\sqrt{m_1^2 - x}\right) - 1$ with x evaluated at $x = 0$; we then conclude from the corresponding asymptotic behaviour that the partial-wave amplitude must have a branch point at $j = \ell_1 + \alpha_2\left((\sqrt{s} - m_1)^2\right) - 1$ which, for $s > s_C$, appears on the physical j sheet.

FOOTNOTES AND REFERENCES

1. D. Amati, S. Fubini, and A. Stanghellini, Phys. Letters 1, 29 (1962); Nuovo Cimento 26, 896 (1962).

2. S. Mandelstam, Nuovo Cimento 30, 1127, 1148 (1963).

3. Mandelstam's analysis of the diagram of Fig. 2 is still only approximate, since he considered only the contribution to the s-channel unitarity relation coming from the three-body intermediate state in which one pair of particles interact to form a Regge pole.

4. C. Wilkin, Nuovo Cimento 31, 377 (1964).

5. V. N. Gribov, I. Ya. Pomeranchuk, and K. A. Ter-Martorosyan, Phys. Rev. 139, B184 (1965); see also Ya. I. Azimov, A. A. Ansel'm, V. N. Gribov, G. S. Danilov, and I. T. Dyatlov, Soviet Phys.-JETP 21, 1189 (1965).

6. The general form of the Regge pole unitarity condition proposed in Ref. 5 has been confirmed by Polkinghorne, using single Regge pole insertions in the Froissart-Gribov continuation, and with the help of some results from perturbation-theory models; see J. C. Polkinghorne, J. Math. Phys. 6, 1960 (1965).

7. Yu. A. Simonov, Soviet Phys.-JETP 21, 160 (1965).

8. J. C. Polkinghorne, J. Math. Phys. 4, 1396 (1963).

9. The methods of Refs. 6 and 8 have further been applied by P. Osborne and J. C. Polkinghorne to the analysis of more general type of Regge pole insertions (Cambridge preprint, 1966).

10. The approximation to the diagram of Fig. 7, which gives rise to the Glauber shadow term, has been discussed by E. S. Abers, H. Burkhardt, V. L. Teplitz, and C. Wilkin, CERN preprint (1965).

11. See the appendix of Ref. 2, p. 1141.

12. We refer to the amplitudes obtained by an approximation of this type as "AFS amplitudes."

13. Whenever there is no confusion possible, we suppress the argument of the trajectory function $\alpha(u)$; we also omit all $(\pm)$ signature lebels if they are not pertinent to the discussion.

14. For small scattering angles the quantity k_z is the z component of $\vec{k}_3$ in the c.m. system of the t reaction, with the z axis taken perpendicular to the direction of the incident momentum $\vec{p}_1$ in the plane formed by the vectors $\vec{p}_1$ and $\vec{q}_1$.

15. To obtain the form (II.12a) we have replaced the original contour in the u plane, which extends along the negative u axis and encircles the branch point at $u = x$, by a fixed contour that encloses the point $u = 0$. This is always possible, since nowhere in the integration region are we forced to distort this contour from its fixed position. Subsequent interchange of the x and u integrations results in formula (II.12a).

16. S. Mandelstam, Nuovo Cimento 30, 1113 (1963).

17. The reader may omit the remainder of this section, since the function $c(u,s)$ is evaluated later; the discussion at this point merely serves as an additional check on the results to be obtained in a subsequent section.

18. If we cut the u plane from $u = 0$ along the negative u axis, then the "leading sheet" is that one which contains the contour C_u.

19. This follows from the fact that the coefficients of the invariant masses which appear in the Feynman denominator function, $D(\alpha, s, t, p_i^2)$, are nonnegative; see N. Nakanishi, Progr. Theoret. Phys., Suppl. 18, (1961).

20. We shall omit throughout this section the signature factors associated with the Regge amplitudes, as well as all $(\pm)$ signature labels.

21. As before, the quantity ℓ should not in general be identified with the total angular momentum j appearing in (I.6); one may interpret it as the total angular momentum, in the s channel, obtained by coupling the (complex) spins of the two Regge poles to a relative orbital angular momentum $L = -1$.

22. The amplitudes A and R are related to the T-matrix element by

$$T_{fi} = (2\pi)^4 \, \delta^4(P_f - P_i) \, \frac{F_{fi}}{[(2\pi)^{3/2}]^4 \prod_{i=1}^{4} \sqrt{2\omega_i}} ,$$

where $F = A$, or R.

23. S. Mandelstam, Phys. Rev. 115, 1741 (1959).

24. H. J. Rothe, Phys. Rev. 140, B1421 (1965).

25. For a discussion of the coupling strength that is required to produce a bound state of zero mass and unit spin in the ladder approximation to the Bethe-Salpeter equation, see: C. Schwartz, Phys. Rev. 137, B717 (1965). It has been shown subsequently by W. B. Kaufmann (priviate communications) that this bound state lies on the leading Regge trajectory.

FIGURE CAPTIONS

Fig. 1. Box diagram in which one of the elementary lines has been replaced by a Regge pole (denoted by a wiggly line); it does not have the AFS-type singularities.

Fig. 2. The analog of Fig. 1, which has the Mandelstam singularity.

Fig. 3. Box diagram in which two of the elementary lines have been replaced by Regge poles; it does not have the singularity proposed by AFS. The AFS approximation consists in taking only the elastic contribution to the unitarity relation (as indicated by the dashed line).

Fig. 4. The analog of Fig. 3, which has the Mandelstam singularity.

Figs. 5 and 6. Diagrams which do not have Mandelstam-type singularities.

Fig. 7. Diagram which contributes to the scattering of particle X from the deuteron, D, and which in the three-body unitarity approximation gives rise to the Glauber shadow term; the symbols p and n stand for the proton and neutron, respectively.

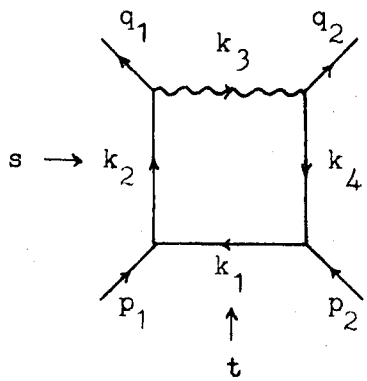

Fig. 1

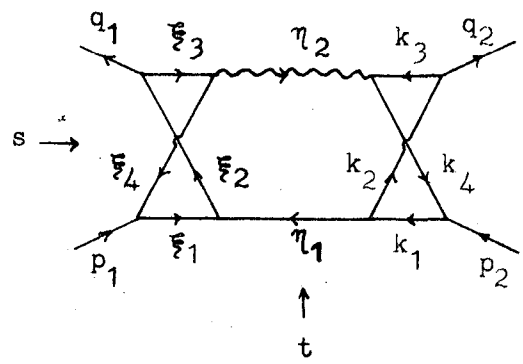

Fig. 2

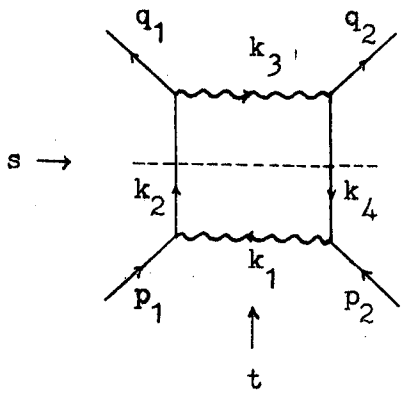

Fig. 3

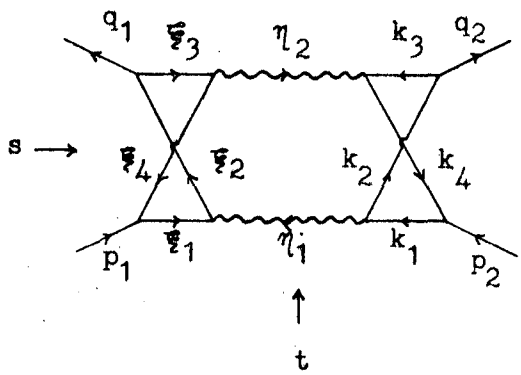

Fig. 4

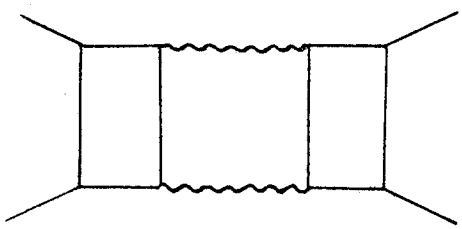

Fig. 5

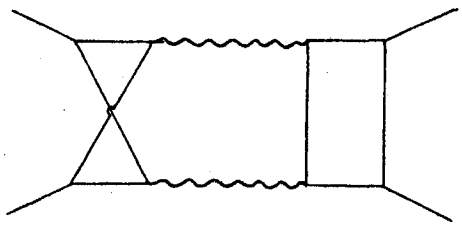

Fig. 6

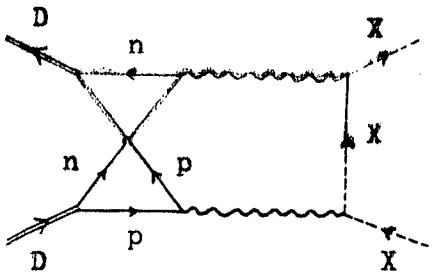

Fig. 7

Fig. 8. Contour in the complex angular momentum plane associated with the background term in the Sommerfeld-Watson representation; $b^{\pm}(s)$ and $\alpha^{\pm}(s)$ are the positions of a branch point and a Regge pole of the continued partial-wave amplitude, $b^{\pm}(j,s)$ [in the figures the symbol $\underline{|x}$ will indicate that we are dealing with the complex "x plane"].

Fig. 9. The shaded area is the domain of integration of the integrand in (I.8); the equation for the boundary is given by $s^2 + s'^2 + s''^2 - 2ss' - 2ss'' - 2s's'' = 0$.

Fig. 10a. The integration contour of (II.10) in the k_z plane for $s < m^2 - x$; we have displaced it slightly into the upper half plane to facilitate the discussion of the integral; $k_{\pm} = \sqrt{-s} \pm i\sqrt{m^2 - x}$ gives the position of the singularities of the integrand arising from the Feynman propagator (shown in the figure for $s < 0$), while $\pm k_B$ and $\pm k_R$ give the locations of the poles arising from the vanishing of $\sin \pi\alpha(x - k_z^2)$ at a bound state of mass $\sqrt{u_B}$ and a resonance of mass $\sqrt{u_R}$; here $k_{B,R} \equiv i\sqrt{u_{B,R} - x}$. The resonance poles, $\pm k_R$, are reached by going through the neighbouring cuts, which are associated with the image of the normal threshold singularities of $\alpha(u)$ and $\gamma(u)$ at $u = u_N$ $(N = 0,1,2\cdots)$ in the k_z plane; in the figure we have also shown the singularities at $\pm k_0 = \pm i\sqrt{u_0 - x}$ which arise from the lowest normal threshold.

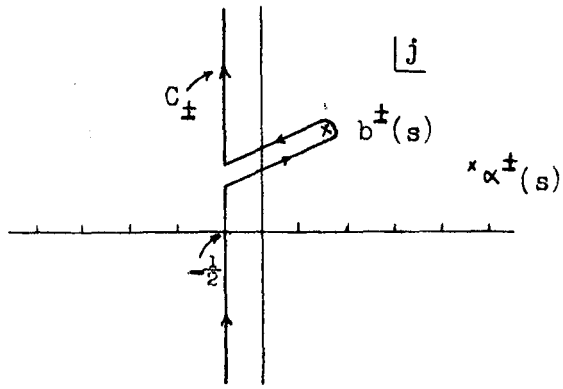

Fig. 8

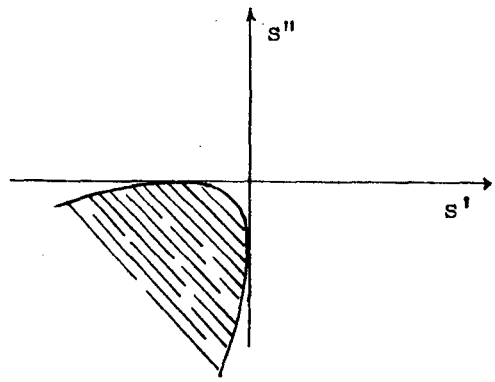

Fig. 9

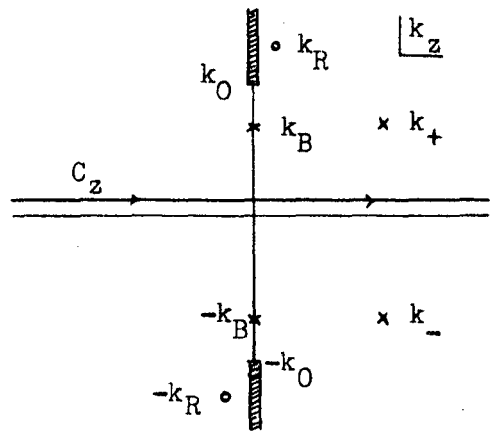

Fig. 10a

Fig. 10b. The integration contour of (II.10) in the k_z plane for $s > m^2 - x$, where $\sqrt{-s}$ has been continued to $s > 0$ according to $\sqrt{-s} = i\sqrt{s}$. For the sake of clarity, only the singularities at $k_z = k_\pm$ are shown in the figure; here k_+ and k_- are defined as in Fig. 10a, with $\sqrt{-s} \to i\sqrt{s}$.

Fig. 10c. Same as in Fig. 10b, except $\sqrt{-s}$ has been continued to $s > 0$ according to $\sqrt{-s} = -i\sqrt{s}$.

Fig. 11. The complex u plane, showing the integration contour C_u for the integral (II.12a); we have not shown the singularities of the integrand.

Figs. 12a,b. The contour C_u of Fig. 11 as it appears in the ℓ plane for $s < m^2$ (Fig. 12a)and for $s > m^2$ (Fig. 12b). Only the singularities that determine the asymptotic behaviour of the AFS amplitude are shown.

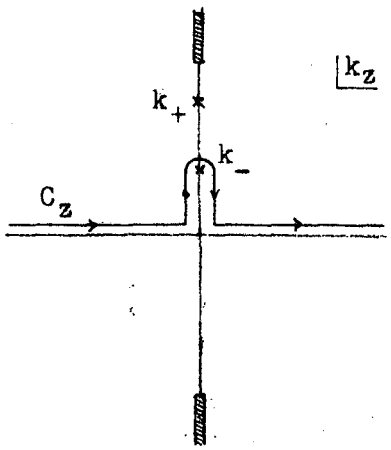

Fig. 10b

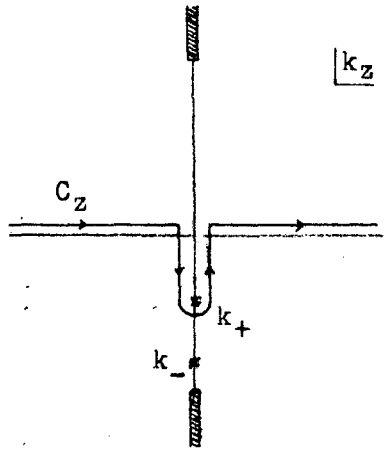

Fig. 10c

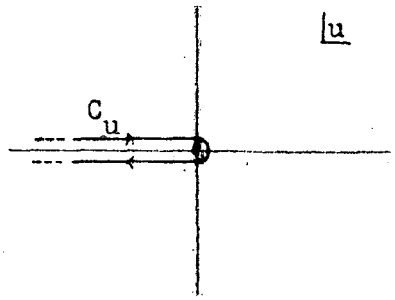

Fig. 11

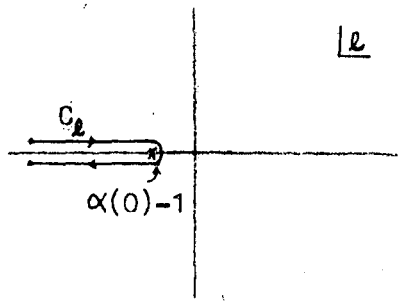

Fig. 12a

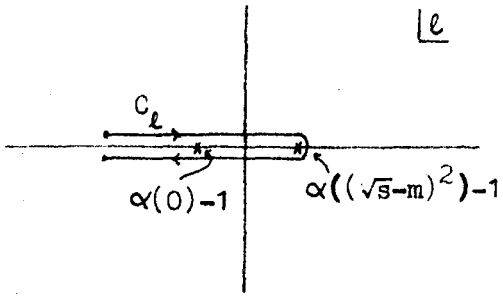

Fig. 12b

Figs. 13a through 18a. Various paths of continuation in the u plane leading from the point u_0 (lying just above the negative axis on the "leading sheet") to the possible singular points of $c(u,s)$ at $u = u_\pm$, where $u_\pm = (m \pm i\sqrt{-s})^2$.

Figs. 13b(c) through 18b(c). The integration contours in the x plane as they appear after the continuation of (II.14a) in u along the various paths shown in Figs. 13a through 18a. The motion of the pole at $x = x_P(u,s)$ is shown by the dashed curves, with $x_0 \equiv x_P(u_0,s)$ as starting point.

Figs. 19a,b through 24a,b. Same as in Figs. 13 through 18, but for $s > 0$; here $u_\pm = (\sqrt{s} \pm m)^2$.

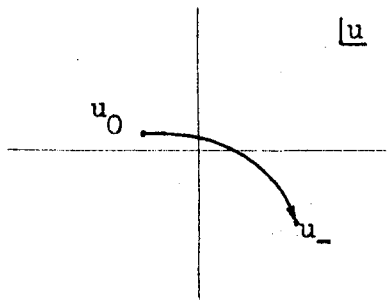

Fig. 13a

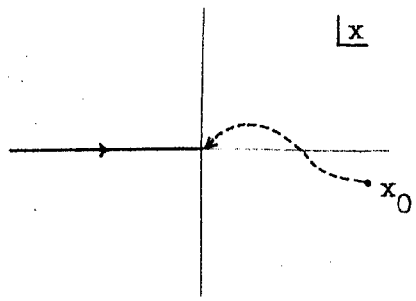

Fig. 13b

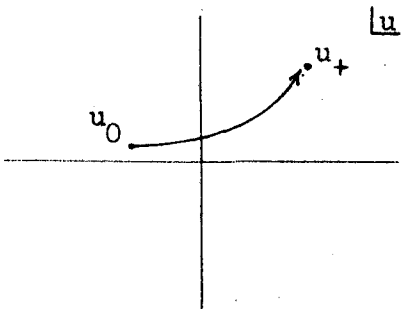

Fig. 14a

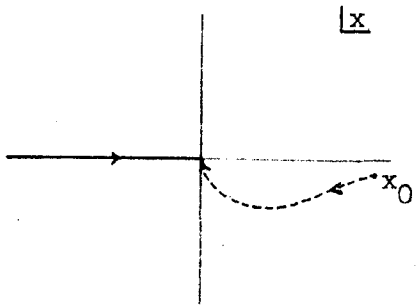

Fig. 14b

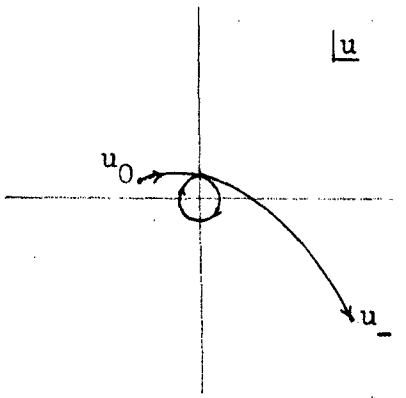

Fig. 15a

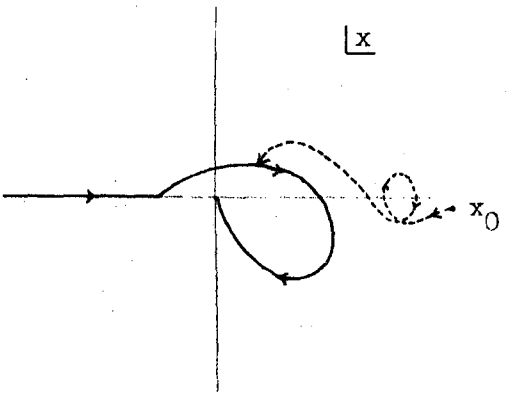

Fig. 15b

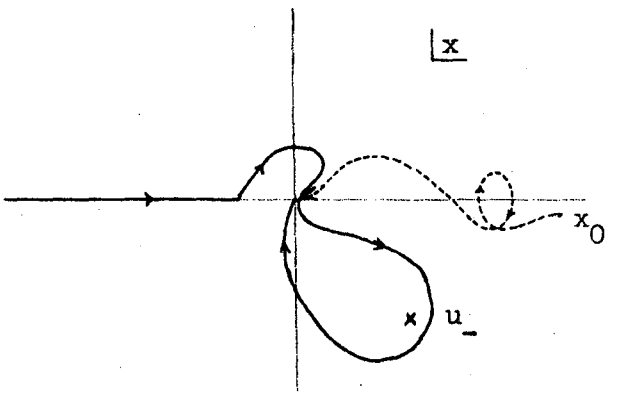

Fig. 15c

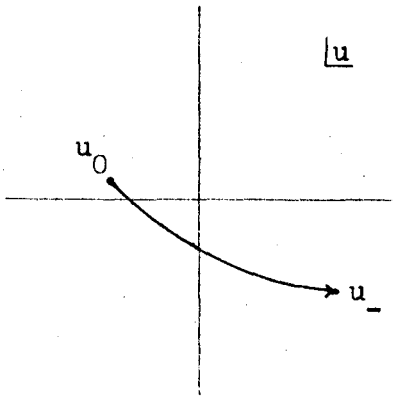

Fig. 16a

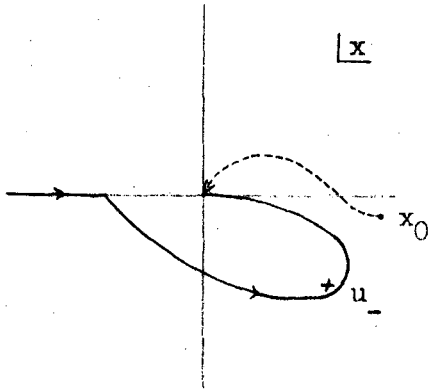

Fig. 16b

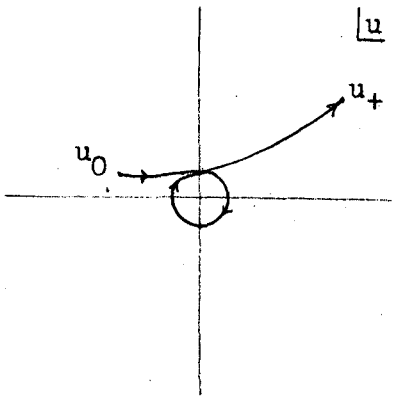

Fig. 17a

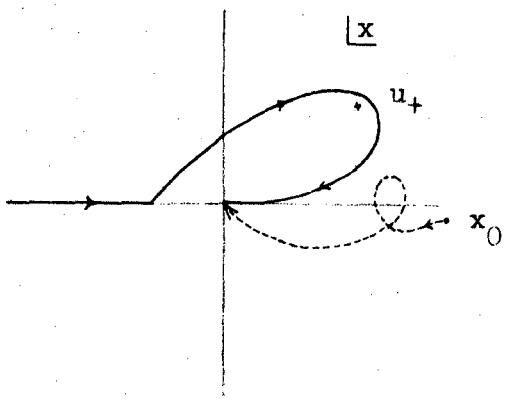

Fig. 17b

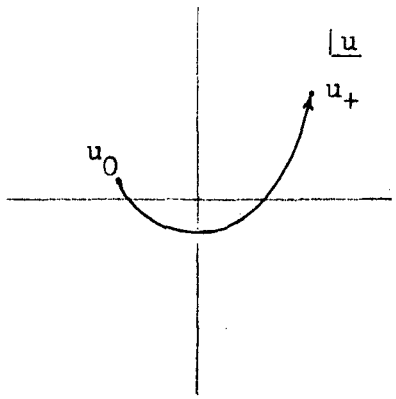

Fig. 18a

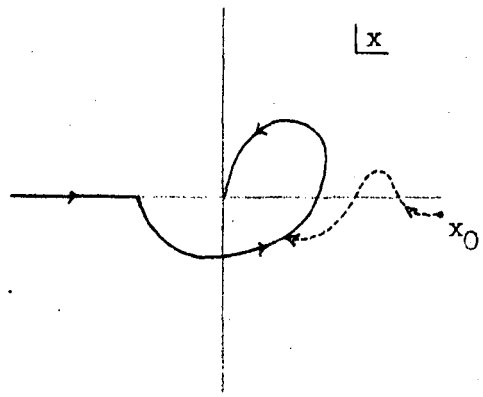

Fig. 18b

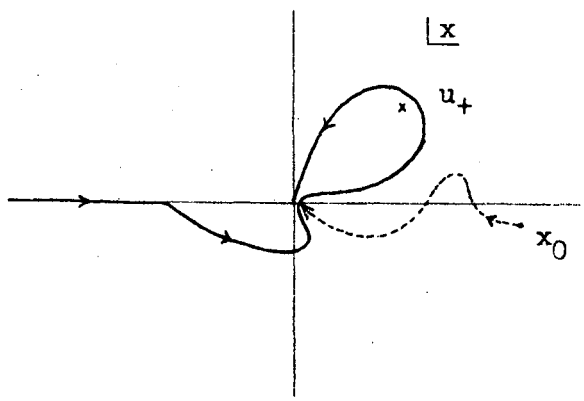

Fig. 18c

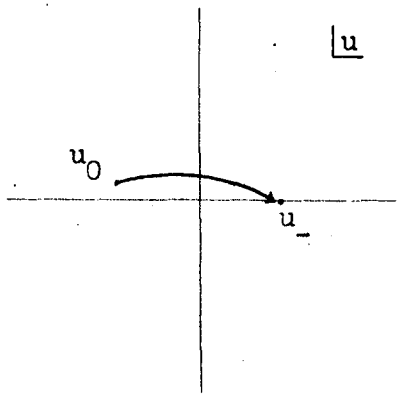

Fig. 19a

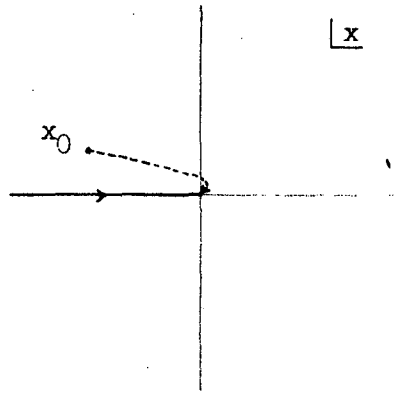

Fig. 19b

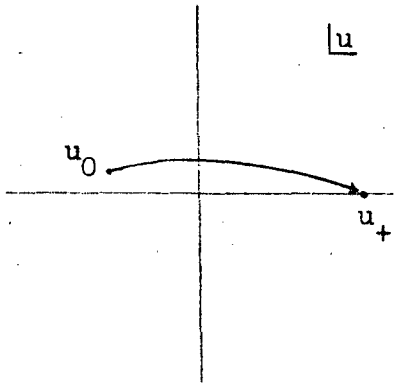

Fig. 20a

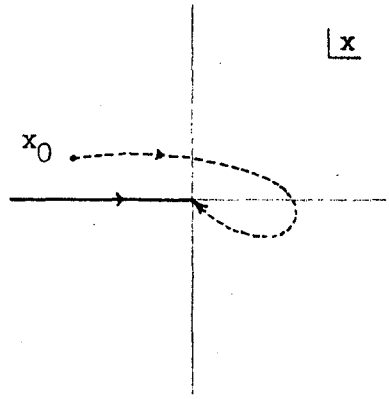

Fig. 20b

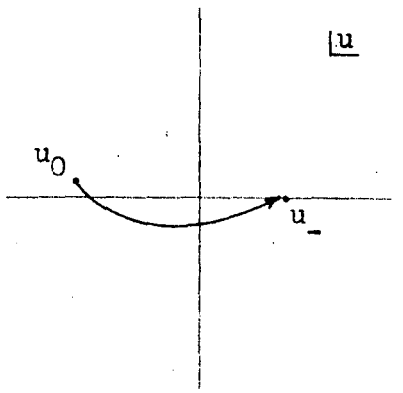

Fig. 21a

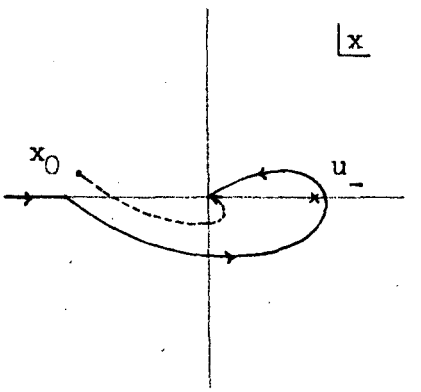

Fig. 21b

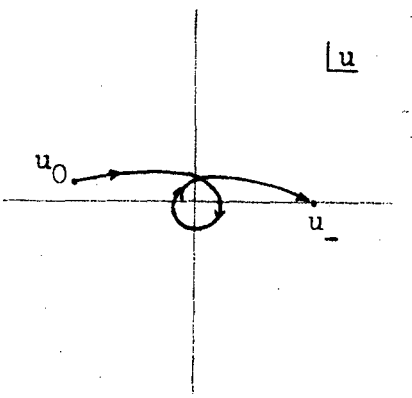

Fig. 22a

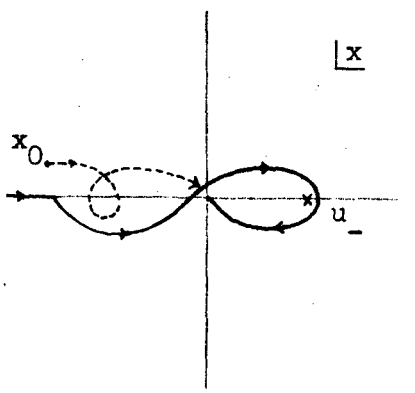

Fig. 22b

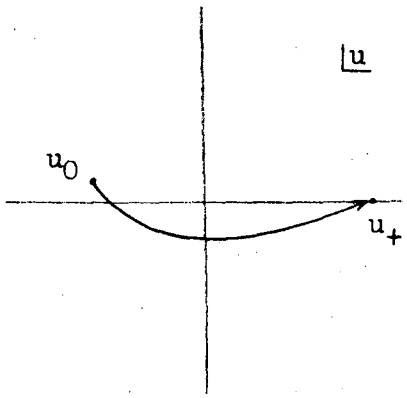

Fig. 23a

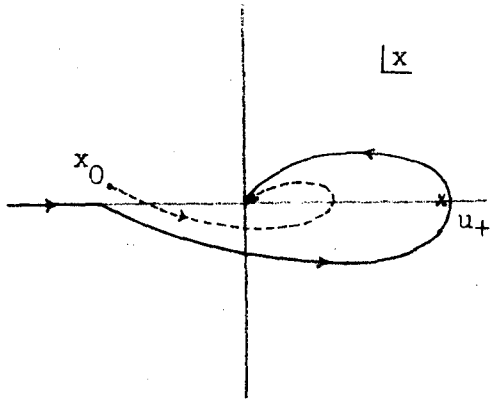

Fig. 23b

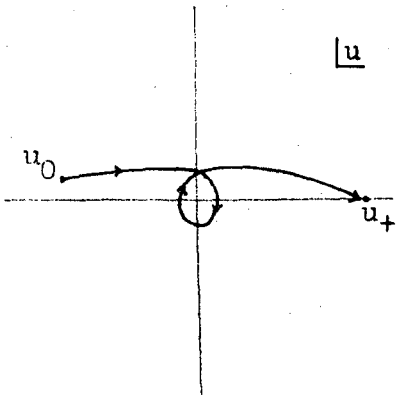

Fig. 24a

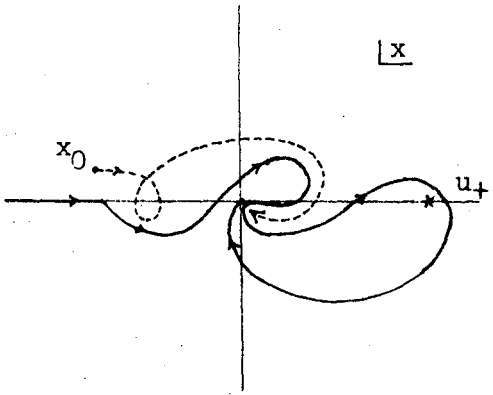

Fig. 24b

Fig. 25. The integration contour C_ℓ of (II.13) for the case in which $\alpha(u) = \frac{1}{2}(3 - \sqrt{4 - u})$; "I" and "II" label the regions of the complex ℓ plane corresponding to the two sheets of $\alpha(u)$ [the dashed line is the dividing line for the two regions]; the singularity of $c(u,s)$ at $u = 0$ is imaged in the ℓ plane as a pair of singularities located at $\ell = -1/2$ and $\ell = 3/2$; the contour C_ℓ encloses only one of these.

Figs. 26,a,b. The integration contour for the integral (II.18) as it appears after continuation of the integral to $s > m^2$; the solid contour (Fig. 26a) corresponds to the case in which the continuation in s has been effected along a path passing below the point $s = m^2$, while the dashed contour (Fig. 26b) corresponds to the case in which the path of continuation lies above $s = m^2$; both continuations lead to the same expression for the AFS amplitude.

Figs. 27a,b. The complex u plane, showing the path P (Fig. 27a) and the path P' (Fig. 27b) along which the discontinuities of $I(u,s)$ are evaluated. The point $u_0 + i\epsilon$ is located on the "leading" logarithmic sheet.

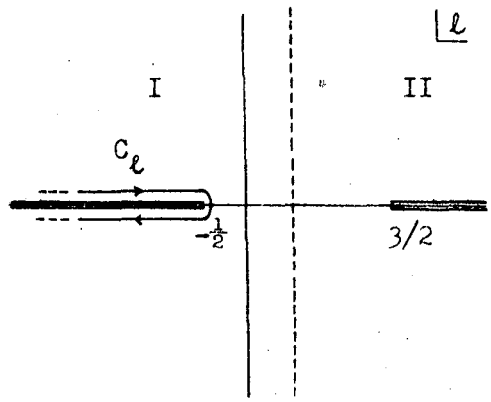

Fig. 25

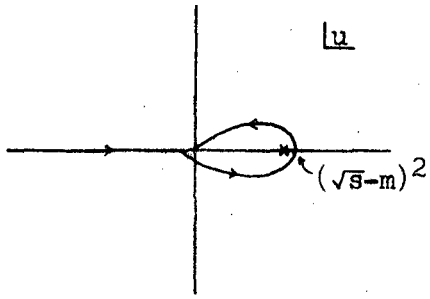

Fig. 26a

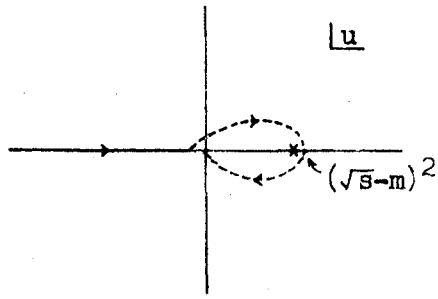

Fig. 26b

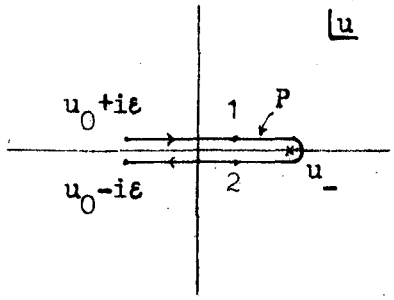

Fig. 27a

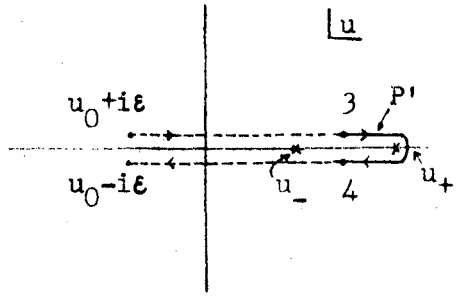

Fig. 27b

Figs. 28a,b,c. Paths leading from the point $A \equiv u_0 + i\epsilon$, located on the leading sheet, to regular points of $I(u,s)$ at $u = u_+$ and $u = u_-$ for the cases $s < 0$ (Fig. 28a), $0 < s < m^2$ (Fig. 28b), and $s > m^2$ (Fig. 28c). The solid and dashed curves correspond to the two choices for the continuation of $\sqrt{-s}$ to $s > 0$: $\sqrt{-s} = i\sqrt{s}$ (solid), $\sqrt{-s} = -i\sqrt{s}$ (dashed).

Fig. 29. The contour C_u in (II.32) split up into two pieces, C' and C''; only the latter contour will be pinched by the moving singularity at $u = (\sqrt{s} - m)^2$ and the pole at $u = M^2$.

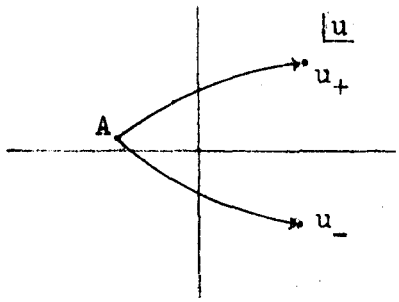

Fig. 28a

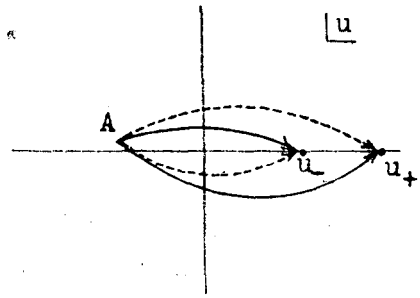

Fig. 28b

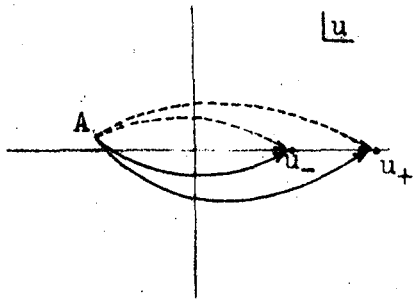

Fig. 28c

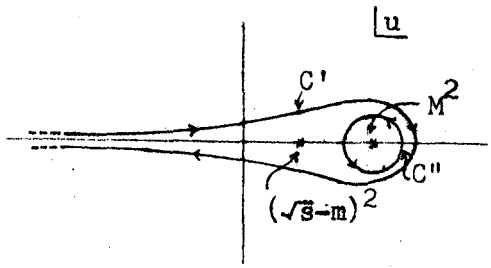

Fig. 29

Fig. 30a. The integration contour of the integral (II.35) in the k_2^2 plane; the point $a - i\mu$ is a singular point of the Regge pole amplitude.

Fig. 30b. The contour C_2 of Fig. 30a split up into C_{AFS} and C'_{AFS} ; the contribution to (II.35) coming from C_{AFS} corresponds to an AFS type of approximation and is precisely cancelled by the contribution from C'_{AFS} .

Fig. 31a. The complex r plane, showing the integration contour C_r of (III.4a) and the singularities of the integrand, for $s < 0$; the pairs of singularities arising from a bound state of mass M and a resonance of mass M_R which lie on the trajectory $\alpha(u)$ are denoted by, $(r_B, \tilde{r}_B)$, $(r'_B, \tilde{r}'_B)$, and $(r_R, \tilde{r}_R)$, $(r'_R, \tilde{r}'_R)$, respectively; they correspond to the various combinations in (III.5) for which $u_N = M^2$ or M_R^2 . The primed and unprimed quantities refer to singularities arising from the individual Regge pole amplitudes. The resonance singularities are reached by going through the neighbouring cuts. Also shown are the singularities arising from the lowest normal threshold branch point of $\alpha(u)$ and $\gamma(u)$ at $u = u_0$; once again they correspond to the various combinations in (III.5) with $u_N \to u_0$.

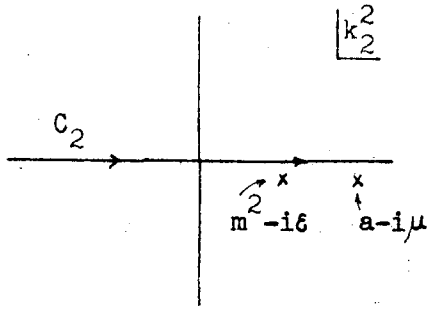

Fig. 30a

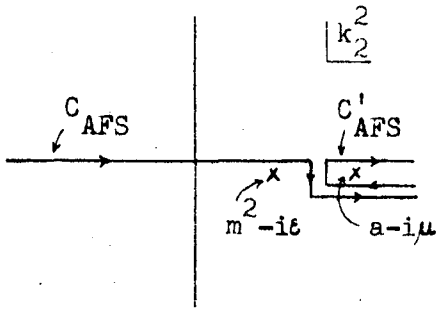

Fig. 30b

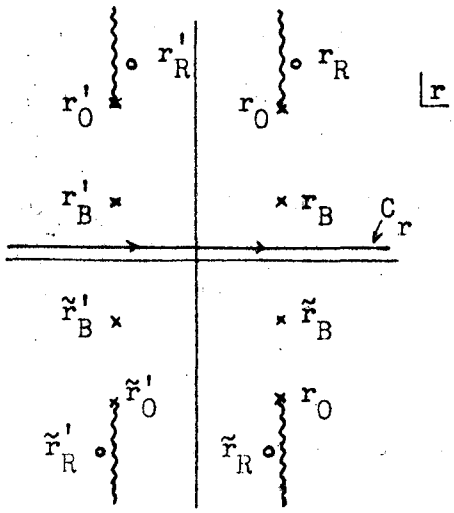

Fig. 31a

Fig. 31b. The contour C_r of Fig. 31a mapped into the complex ℓ plane. Only the singularity at $\ell = 2\alpha(x + s/4) - 1$ of the integrand of (III.7), which arises from the vanishing of $\partial\ell/\partial r$, is shown.

Figs. 31c,d. The contour C_r of Fig. 31a, and the singularities arising from the bound state of the Regge pole as they appear for $0 < s < 4M^2 - x$, (Fig. 31c), and for $s > 4M^2 - x$ (Fig. 31d), where M is the mass of the bound state.

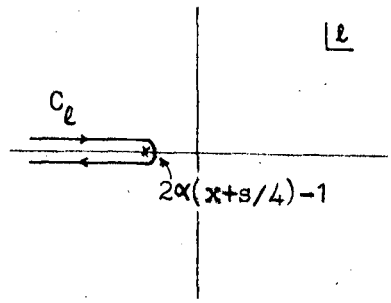

Fig. 31b

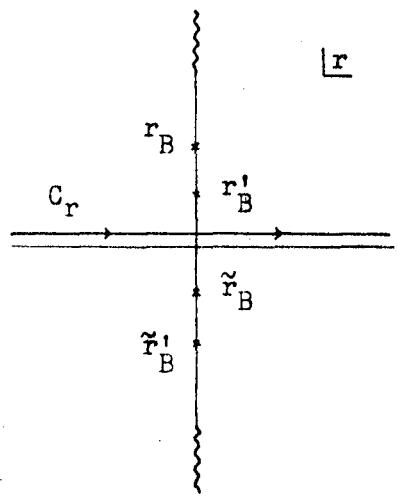

Fig. 31c

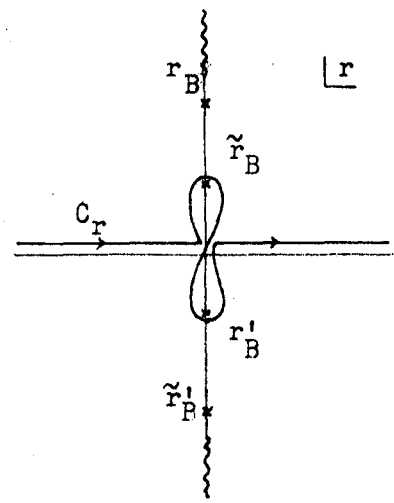

Fig. 31d

Figs. 32a,b. The contracted Feynman diagrams associated with the left-hand cross in Fig. 2.

Figs. 33a,b. The original integration contour of (IV.12b) in the t' plane (Fig. 33a), and the equivalent contour, which extends around the t-channel threshold cut of $A^C(s,t)$ [Fig. 33b].

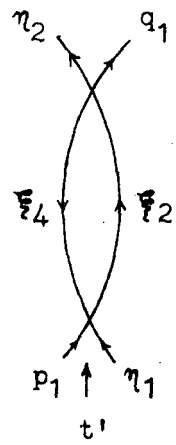

Fig. 32a

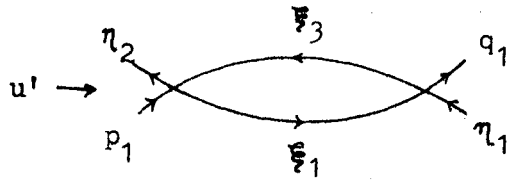

Fig. 32b

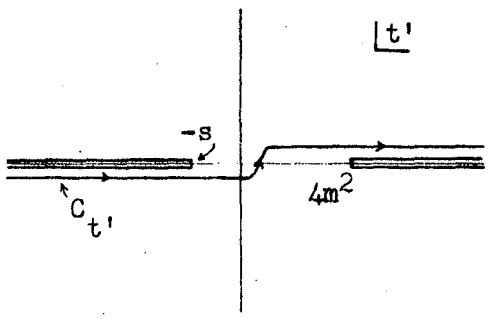

Fig. 33a

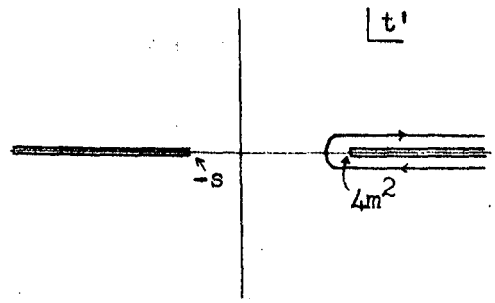

Fig. 33b

This report was prepared as an account of Government sponsored work. Neither the United States, nor the Commission, nor any person acting on behalf of the Commission:

A. Makes any warranty or representation, expressed or implied, with respect to the accuracy, completeness, or usefulness of the information contained in this report, or that the use of any information, apparatus, method, or process disclosed in this report may not infringe privately owned rights; or

B. Assumes any liabilities with respect to the use of, or for damages resulting from the use of any information, apparatus, method, or process disclosed in this report.

As used in the above, "person acting on behalf of the Commission" includes any employee or contractor of the Commission, or employee of such contractor, to the extent that such employee or contractor of the Commission, or employee of such contractor prepares, disseminates, or provides access to, any information pursuant to his employment or contract with the Commission, or his employment with such contractor.